2014-05-01

Characterization of Cretaceous Chalk Microporosity Related to Depositional Texture: Based Upon Study of the Upper Cretaceous Niobrara Formation, Denver-Julesburg Basin, Colorado and Wyoming

P D. Pahnke
Brigham Young University - Provo

Characterization of Cretaceous Chalk Microporosity Related to Depositional Texture: Based Upon Study of the Upper Cretaceous Niobrara Formation, Denver-Julesburg Basin, Colorado and Wyoming

Peter D. Pahnke

A thesis submitted to the faculty of
Brigham Young University
in partial fulfillment of the requirements for the degree of

Master of Science

Scott M. Ritter, Chair
Thomas H. Morris
Bart J. Kowallis

Department of Geological Sciences

Brigham Young University

May 2014

ABSTRACT

Characterization of Cretaceous Chalk Microporosity Related to Depositional Texture:
Based Upon Study of the Upper Cretaceous Niobrara Formation,
Denver-Julesburg Basin, Colorado and Wyoming

Peter D. Pahnke
Department of Geological Sciences, BYU
Master of Science

Prompted by increased interest in understanding microporosity, recent efforts at describing and classifying pore types in mudstones have focused primarily on siliceous, gas producing unconventional reservoirs with little attention being paid to carbonate, mixed oil-and-gas producers. The Niobrara Formation in the Denver-Julesburg Basin is a self-sourced resource play producing oil and natural gas from low permeability chalks. Key reservoir lithologies consist of chalk, chalky marl and marl. These lithologies contain flattened chalk fecal pellets which play a significant role in providing porosity.

Integration of depositional fabric with pore-type distribution emphasizes the unique textural and depositional nature of chalk and provides a starting point for evaluation of diagenetic porosity modification. Chalk depositional textures comprise two main subdivisions. The first, called *rainstone*, includes chalks that form largely from settling of planktonic skeletal remains and fecal pellets as marine snow. New terms related to pelagic chalk textures are *pelagic mudstone*, *pelagic wackestone*, and *pelagic packstone*. The second, called *allochthonous chalk*, consists of chalks formed from syndepositional tectonic disruption of the seafloor, resulting in mass-movement and redeposition of chalk as turbidites and slide sheets. New terms related to allochthonous chalk textures are *allomudstone*, *allofloatstone,* and *allorudstone*.

A chalk porosity classification consisting of four major pore types is presented that can be used to quantify Niobrara chalk pores and relate them to depositional texture, porosity networks, diagenetic history, and pore distributions. Interparticle porosity occurs largely between coccoliths and coccolith fragments, and decreases with burial ranging from 27-38% to 5-17%. Intraparticle porosity occurs within chalk pellets, coccospheres, coccolith plates and foraminifera tests, and also decreases with burial. Organic matter pores are intraparticle pores located within organic matter and are related to hydrocarbon generation. Channel pores, where present, can have significant influence on hydrocarbon storage and permeability networks.

In the Niobrara, burial diagenesis in the form of mechanical compaction, chemical compaction, and syntaxial cement overgrowths, modifies pore shape and abundance. Porosity distribution is controlled by the abundance of chalk pellets and the mineralogy of the matrix. Permeability is a function of matrix lithology (micrite-rich vs. silt- and clay-rich).

Understanding chalk depositional and diagenetic processes, and how they relate to porosity formation and pore evolution provide a foundation for more accurately predicting the occurrence and distribution of hydrocarbon source and reservoir rocks within the Niobrara.

Keywords: Niobrara, Denver-Julesburg Basin, chalk, rainstone, allochthonous chalk, marl, coccolith, chalk pellet, chalk porosity, chalk diagenesis

ACKNOWLEDGMENTS

I would like to acknowledge and thank the Energy & Geoscience Institute (EGI) for providing funding for this project through their Liquids from Shales Phase 2 project. Special thanks to Dr. Milind Deo, Tom Anderson, Carrie Welker, Bryony Richards-McClung, and Nick Dahdah for their guidance and assistance, along with the 15 corporate sponsors who participated. Special thanks also to the employees of the Utah Nanofab Facility at the University of Utah for use of their SEM equipment, and to Jeffrey Quick from the Utah Geological Survey for sharing his UV fluorescence microscopy expertise.

I would like to express my sincere appreciation to my thesis advisor, Scott Ritter, for giving so much of his time and talents in helping me achieve my goals, and to my thesis committee members, Doc Morris, Bart Kowallis, and other professors who have assisted along the way. Many thanks as well to Geoff Ritter, who assisted with SEM point counting.

I am grateful to have been able to attend Brigham Young University both as an undergraduate and graduate student and wish to express my gratitude to the Department of Geological Sciences. Thank you for the numerous hours spent instructing, molding, building, and teaching me, and for the many world-class field trips and courses I was able to take part in.

Finally, I would like to express heartfelt gratitude for my son, Gavin, for his constant motivation and his ability to brighten my days with his infectious smile, and to my family for their continued encouragement and belief in my talents and abilities.

TABLE OF CONTENTS

LIST OF FIGURES

LIST OF TABLES

Characterization of Cretaceous Chalk Microporosity Related to Depositional Texture: Based Upon Study of the Upper Cretaceous Niobrara Formation, Denver-Julesburg Basin, Colorado and Wyoming

Peter D. Pahnke & Scott M. Ritter

ABSTRACT

Prompted by increased interest in understanding microporosity, recent efforts at describing and classifying pore types in mudstones have focused primarily on siliceous, gas producing unconventional reservoirs with little attention being paid to carbonate, mixed oil-and-gas producers. The Niobrara Formation in the Denver-Julesburg Basin is a self-sourced resource play producing oil and natural gas from low permeability chalks. Key reservoir lithologies consist of chalk, chalky marl and marl. These lithologies contain flattened chalk fecal pellets which play a significant role in providing porosity.

Integration of depositional fabric with pore-type distribution emphasizes the unique textural and depositional nature of chalk and provides a starting point for evaluation of diagenetic porosity modification. Chalk depositional textures comprise two main subdivisions. The first, called *rainstone*, includes chalks that form largely from settling of planktonic skeletal remains and fecal pellets as marine snow. New terms related to pelagic chalk textures are *pelagic mudstone*, *pelagic wackestone*, and *pelagic packstone*. The second, called *allochthonous chalk*, consists of chalks formed from syndepositional tectonic disruption of the seafloor, resulting in mass-movement and redeposition of chalk as turbidites and slide sheets. New terms related to allochthonous chalk textures are *allomudstone*, *allofloatstone,* and *allorudstone*.

A chalk porosity classification consisting of four major pore types is presented that can be used to quantify Niobrara chalk pores and relate them to depositional texture, porosity networks, diagenetic history, and pore distributions. Interparticle porosity occurs largely between coccoliths and coccolith fragments, and decreases with burial ranging from 27-38% to 5-17%. Intraparticle porosity occurs within chalk pellets, coccospheres, coccolith plates and foraminifera tests, and

also decreases with burial. Organic matter pores are intraparticle pores located within organic matter and are related to hydrocarbon generation. Channel pores, where present, can have significant influence on hydrocarbon storage and permeability networks.

In the Niobrara, burial diagenesis in the form of mechanical compaction, chemical compaction, and syntaxial cement overgrowths, modifies pore shape and abundance. Porosity distribution is controlled by the abundance of chalk pellets and the mineralogy of the matrix. Permeability is a function of matrix lithology (micrite-rich vs. silt- and clay-rich).

Understanding chalk depositional and diagenetic processes, and how they relate to porosity formation and pore evolution provide a foundation for more accurately predicting the occurrence and distribution of hydrocarbon source and reservoir rocks within the Niobrara.

INTRODUCTION

Programs for exploration of oil and gas in carbonate rocks are based in part upon understanding the geometry and genesis of pore systems. The three most widely used schemes for classifying pore systems are from Choquette and Pray (1970), Lucia (1983, 1995), and Lønøy (2006). Choquette and Pray's (1970) transformative classification emphasized the evolution of carbonate pore systems from original sediment to solid rock under the influence of marine, meteoric, and connate waters and elucidated for the first time the broad range of pore types that characterize carbonate reservoirs relative to their sandstone counterparts. Their scheme is particularly useful to exploration geologists with access to rock samples and with a goal of understanding basin histories.

For petrophysicists and production geoscientists, the Lucia (1983, 1995) porosity scheme was a welcome alternative to that of Choquette and Pray (1970) because pore types were directly tied to petrophysical parameters that could be used to predict reservoir performance. The petrophysical classification presented by Lucia (1983) was based upon a comparison of rock-fabric descriptions with laboratory measurements of porosity, permeability, capillarity, and Archie *m* values (cementation exponent). The basis of the Lucia (1983) classification is

the concept that pore-size distribution controls permeability and saturation and that pore-size distribution is related to rock fabric. Lab measurements were used to define three rock-fabric classes that correspond to a modified version of Dunham's (1962) textural classification of limestone. This classification enables reservoir engineers to integrate petrophysics with depositional and stratigraphic models to predict porosity and permeability trends away from the well bore.

Lønøy (2006) evaluated data from approximately 3000 carbonate plug samples representing a wide range of geological ages and sedimentary basins and found a poorly defined empirical relationship between measured porosity/permeability and some of the previously defined pore types. Therefore, he proposed a new system of 20 pore types that 1) improved coefficient of determination values (R^2) for porosity and permeability within each pore-type category and that 2) permitted improvements in correlation of porosity cutoff values and permeability prediction. Lønøy's scheme uses concepts from Choquette and Pray (1970) and from Lucia (1983, 1995) in addition to many new elements (Figure 1). Important additions to the classification include the identification of uniform and patchy porosity distributions, measurement of pore diameters, and, most germane to this paper, the incorporation of a new mudstone microporosity class that includes Cretaceous and Tertiary chalks.

The current emphasis on unconventional reservoirs has created a need to better understand microporosity and effective permeability pathways within carbonate mudstones. The purpose of this study is to expand and enhance Lønøy's (2006) mudstone microporosity pore-type class, specifically the Cretaceous chalk subclass, by documenting the pore types, networks and diagenetic effects found among the primary constituents of the Cretaceous Niobrara Formation across the Denver-Julesburg (DJ) Basin.

The Niobrara is an evolving hydrocarbon-producing play in low permeability chalk and marl sequences. Still in the early stages of study and development as an unconventional resource, it lacks detailed investigation of basic pore characteristics vital to understanding and predicting reservoir producibility. Specific study objectives are to 1) evaluate the relationship between

Pore Type	Pore Size	Pore Distribution	Pore Fabric	R^2
Interparticle	Micropores (10–50 μm)	Uniform	Interparticle, uniform micropores	0.88
		Patchy	Interparticle, patchy micropores	0.79
	Mesopores (50–100 μm)	Uniform	Interparticle, uniform mesopores	0.86
		Patchy	Interparticle, patchy mesopores	0.85
	Macropores (>100 μm)	Uniform	Interparticle, uniform macropores	0.88
		Patchy	Interparticle, patchy macropores	0.87
Intercrystalline	Micropores (10–20 μm)	Uniform	Intercrystalline, uniform micropores	0.92
		Patchy	Intercrystalline, patchy micropores	0.79
	Mesopores (20–60 μm)	Uniform	Intercrystalline, uniform mesopores	0.94
		Patchy	Intercrystalline, patchy mesopores	0.92
	Macropores (>60 μm)	Uniform	Intercrystalline, uniform macropores	0.80
		Patchy	Intercrystalline, patchy macropores	
Intraparticle			Intraparticle	0.86
Moldic	Micropores (<10–20 μm)		Moldic micropores	0.86
	Macropores (>20–30 μm)		Moldic macropores	0.90
Vuggy			Vuggy	0.50
Mudstone microporosity	Micropores (<10 μm)		Tertiary chalk	0.80
			Cretaceous chalk	0.81
		Uniform	Chalky micropores, uniform	0.96
		Patchy	Chalky micropores, patchy	

Figure 1. Lønøy's (2006) carbonate pore classification scheme.

chalk lithology and chalk microporosity; 2) classify Niobrara chalk micropores; 3) examine and compare porosity types in the main Niobrara lithologies; 4) evaluate the effects of diagenesis on pore modification; 5) discuss the nature, origin, and importance of uniform vs. patchy pore distributions. This study is restricted to available data. It is based on core and outcrop samples collected from the Niobrara 'B' chalk and marl across the DJ Basin.

GEOLOGIC BACKGROUND

The Niobrara Formation is a self-sourced petroleum resource play currently producing oil and natural gas from low permeability chalks and marls (Sonnenberg, 2011b). Found throughout much of the Rocky Mountain Region, it was deposited along the eastern margin of the Western Interior Cretaceous Seaway (WICS) (Figure 2), an asymmetric foreland basin, during the maximum transgressive phase of the Niobrara Cyclothem (early Coniacian though early Campanian) (Barlow and Kauffman, 1985; Longman et al., 1998).

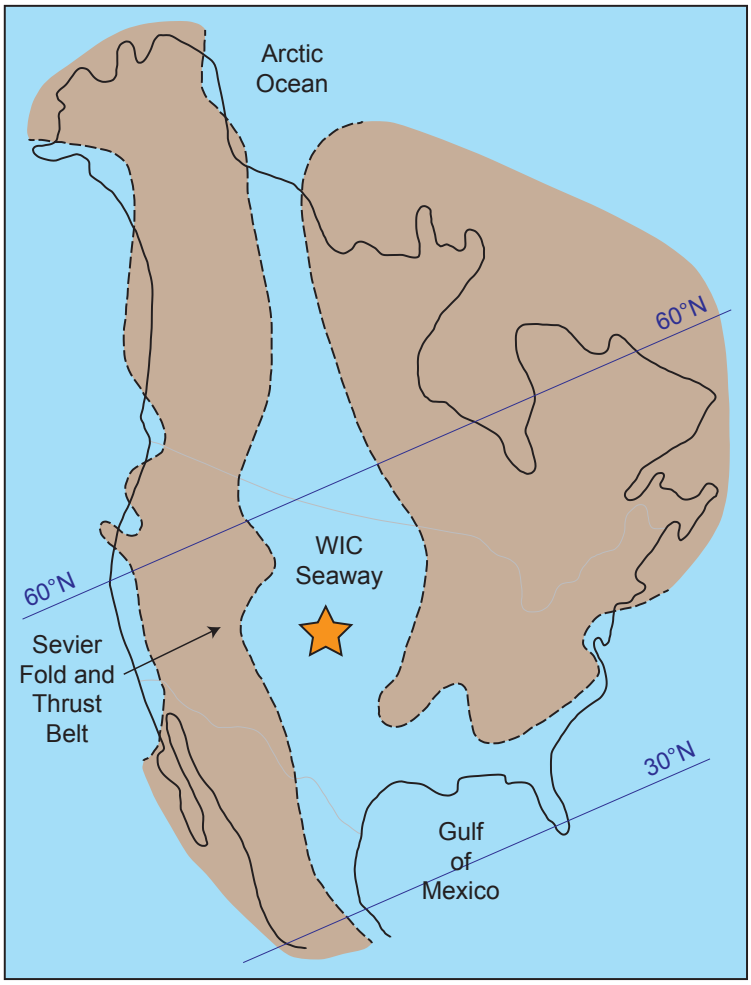

Figure 2. Figure showing the Western Interior Cretaceous Seaway (WICS) during Niobrara deposition. The source area for clastic sediments is predominantly to the west and is related to the Sevier Fold and Thrust Belt. Total organic content (TOC) increases to the east where carbonate content is generally higher. Figure modified from Sonnenberg (2011).

The Niobrara Formation overlies the Codell Sandstone Member of the Carlile Shale and is overlain by the Pierre Shale. It is subdivided into two members: the Fort Hays Limestone and the Smoky Hill (Figure 3). The Fort Hays is a regionally extensive succession of thick-bedded chalky limestones, ranging in thickness from 50 ft (15 m) in southeast Colorado to 120 ft (36 m) in New Mexico and less than 10 ft (3 m) in Wyoming (Sonnenberg, 2011b). The overlying Smoky Hill Member consists of three interbedded organic-rich chalk-marl sequences named, in descending stratigraphic order, the A, B, and C. Principal lithologies of the Smoky Hill are chalk, chalky marl and marl with thicknesses ranging from 100 to 300 ft (30 to 90 m) along the eastern margin of the DJ Basin to over 1500 ft (450 m) in western Colorado and eastern Utah (Longman et al., 1998). Primary constituents of the Smoky Hill include coccolith-rich chalk fecal pellets, planktonic foram tests, oyster and inoceramid shell fragments, micrite-grade shields and

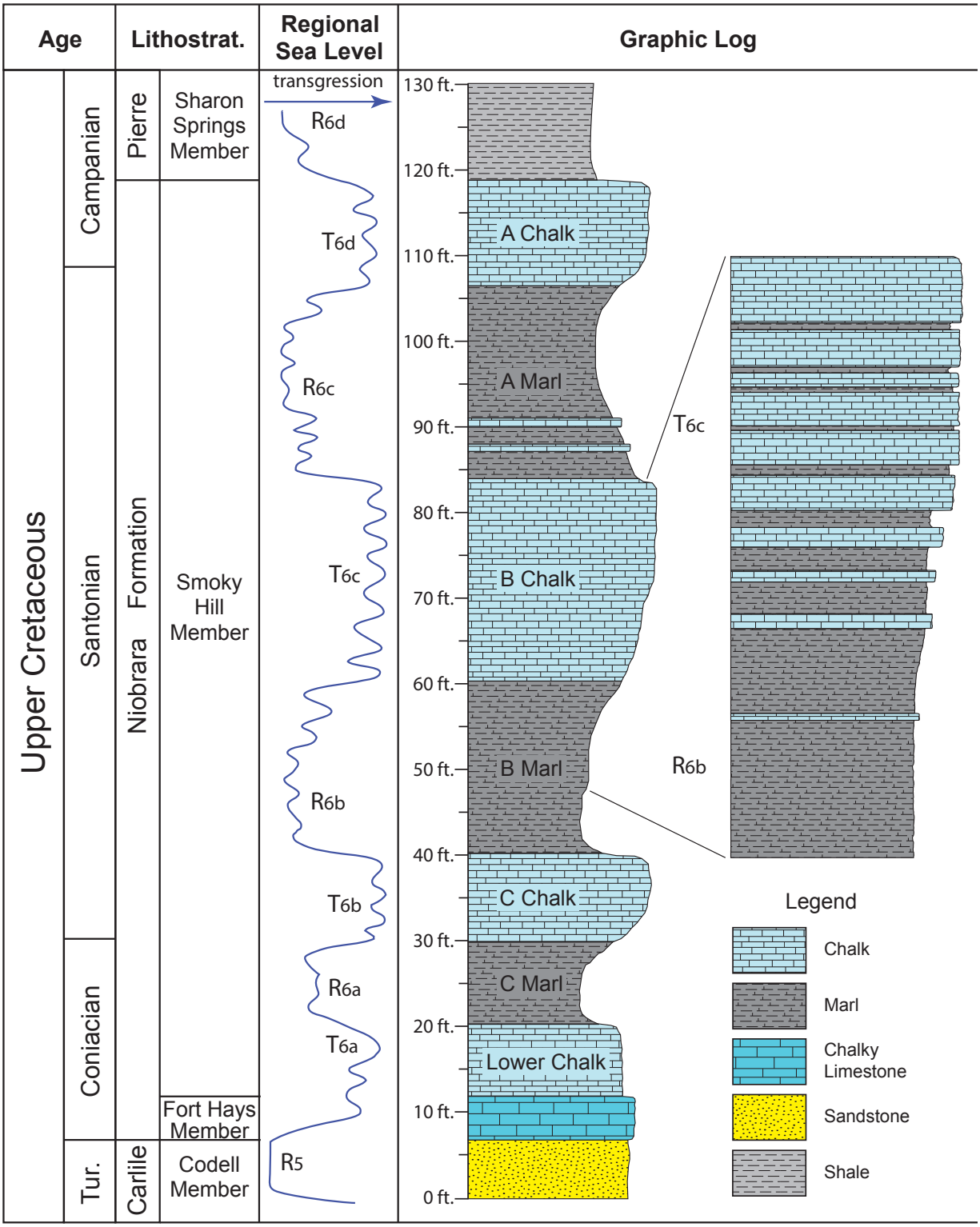

Figure 3. Stratigraphic column of the Niobrara Formation at 6 Mile Fold, north of Boulder, Colorado showing the Fort Hays Limestone and the chalk-marl sequences of the Smoky Hill Member. The column of the right zooms in on the 'B' interval providing additional detail. Regional sea level curve modified from Kauffman and Caldwell (1993). Figure after Longman et al. (1998) and Gustason and Deacon (2010).

fragments of coccoliths, clay, quartz silt, pyrite framboids and organic matter. Setting it apart from other chalk formations, much of the Smoky Hill section is composed of chalk fecal pellets mostly likely produced by pelagic copepods (Hattin, 1975; Longman et al., 1998). These chalk pellets have been flattened by burial, but are otherwise preserved nearly intact. Similar pellets occur locally within the Austin Chalk, but are not as common or well preserved because of extensive bioturbation (Longman et al., 1998).

The Niobrara Formation is an emerging unconventional resource play requiring horizontal drilling and multi-stage hydraulic fracturing to economically produce oil and gas. Source rocks contain mostly Type II (sapropelic) oil-prone kerogens and source rocks are reported as having organic content ranging from 0.5 to 8.0 wt. % (Landon et al., 2001). Oil accumulations occur where source rocks are currently in the thermal maturity oil window and the 'B' interval is currently the main production target.

DATA AND METHODS

As part of this study, core and outcrop samples from eight Niobrara Formation localities were analyzed petrologically using thin section, QEMSCAN® and Scanning Electron Microscope (SEM) analyses (Figure 4). Core samples were collected from wells in Laramie County, Wyoming, from Weld County and Yuma County, Colorado and from Sherman County, Kansas (Table 1). Outcrop samples were collected at Six Mile Fold, north of Boulder, Colorado, at Laporte Quarry, north of Laporte, Colorado and at Sage Creek, south of Rawlins, Wyoming. Great effort was made to obtain samples representing each stratigraphic interval as well as distinct diagenetic end members.

Thin Section Analysis

Mudstone micropores are not easily observed using standard petrographic thin sections. However, by using thin sections impregnated with blue epoxy in conjunction with an ultraviolet (UV) enhancing dye, we were able to determine the distribution of micropore-rich domains.

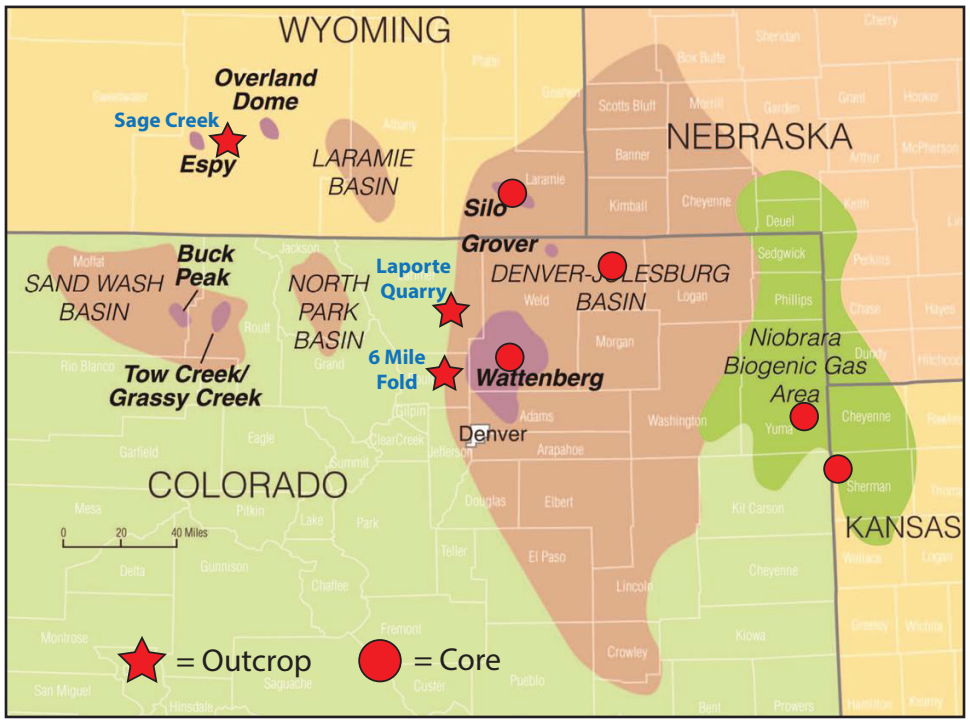

Figure 4. Index map of Colorado, Wyoming, Nebraska, and Kansas showing areas of Niobrara oil and gas production and sample collection localities. Figure modified from Williams and Lyle (2011).

For this study, 60 petrographic thin sections were prepared. In domains of high porosity, a weak bluish hue is visible under normal transmitted light. The same domain under UV light is expressed as bright, fluorescent blue.

QEMSCAN Analysis

QEMSCAN® (Quantitative Evaluation of Minerals using Scanning Electron Microscopy) is a fully automated micro-analysis system that enables quantitative chemical analysis of materials and the generation of high-resolution mineral maps and images (Ayling et al., 2012). It uses an electron beam source in combination with four energy dispersive X-ray spectrometers (EDS) on a scanning electron microscopy (SEM) platform. The measured backscattered electron (BSE) and EDS spectra are used to classify sample mineralogy at each measurement point, comparing recorded values against a mineral Species Identification Program (SIP) library. The identified minerals are then assigned a color and a digital map of the analyzed area is created.

Table 1. List of wells which were sampled for this study

WELL	API #	COUNTY	STATE	S-T-R	LATITUDE	LONGITUDE
Combs	49-021-20287	Laramie	Wyoming	35-16N-65W	41.31659	-104.61743
Lee 41-5	49-021-20349	Laramie	Wyoming	5-15N-64W	41.30142	-104.56107
Horse Creek T84X-31G	49-021-20391	Laramie	Wyoming	31-17N-68W	41.40166	-105.03879
Burbach 20-3H	05-123-14883	Weld	Colorado	3-11N-62W	40.95758	-104.30619
Timbro PC LD16-17	05-123-33305	Weld	Colorado	16-9N-58W	40.75352	-103.86409
Aristocrat H11-07	05-123-32394	Weld	Colorado	11-3N-65W	40.24117	-104.62864
Whomble 1-32	05-125-06075	Yuma	Colorado	32-2S-43W	39.84620	-102.20690
Schock Errington 1	15-181-20030	Sherman	Kansas	11-7S-42W	39.46101	-101.97823

QEMSCAN® results provide a range of information including the composition, distribution, fabric and texture of minerals, in addition to depositional environment (e.g., micro-layering and bedding) and maturity of samples etc. QEMSCAN® analyses were run on 10 samples selected to represent the chief lithologies of the Niobrara Formation. They were completed at the Energy & Geoscience Institute (EGI) at the University of Utah using a QEMSCAN® 4300. Samples were set in epoxy and mechanically polished. Measurements were initially collected in low-resolution, field-scan mode at 20 micron spacing. High-resolution 5 micron spacing measurements were then collected on areas of interest. The QEMSCAN® was operated using an accelerating voltage of 20kV and a specimen current of approximately 5.0 nA. Mineral classification was completed using the Oil and Gas Species Identification Protocol (SIP) version 3.3 developed by FEI for fine-grained sediments.

SEM Sample Preparation

The process of mechanical polishing has been known to produce surface topographic irregularities, potentially introducing errors into pore identification using SEM-based imaging techniques (Loucks et al., 2009). Originally called ion thinning, Argon (Ar)-ion milling has been utilized in the physical sciences to produce a surface free of damage caused by mechanical polishing and to enhance surface viewing characteristics since the early 1970s (Brace et al.,

1972; Sprunt and Brace, 1974; Simmons and Richter, 1976). In order to create a surface devoid of major artifacts, eight samples were prepared using Ar-ion milling. Ion-milled samples were prepared using a Fischione Model 1060 SEM Mill located in the Utah Nanofab facility at the University of Utah.

SEM Analysis

Argon-ion milled samples were examined using the FEI Quanta 600, a state-of-the-art SEM with a high-resolution field-emission gun (FEG) source. The Quanta 600 system can operate in high-vacuum, low-vacuum, and in environmental ESEM (water vapor ambient) modes with a practical resolution of approximately 1.4 nm – 3.0 nm. Energy dispersive X-ray Spectroscopy (EDX) is also available for mineral identification. Individual images collected on the Quanta 600 SEM were captured using the secondary electron (SE) detector for viewing topographic features and the backscattered secondary electron (BSE) detector for defining compositional variations. Images were also collected by superimposing SE and BSE detector modes. Lower accelerating voltages (10-15kV) were used to help manage charging and to prevent beam damage to the sample. Working distances were 8 to 10 mm.

To further aid in understanding pores and their distributions, FEI's Modular Automated Processing System or MAPS™ analyses have been collected on samples representing each of the three main Niobrara lithologies. MAPS™ is a fully automated correlative microscopy software package that performs navigation, tiling and stitching of SEM images at high-magnification and high-resolution into composite image mosaics. Viewing an image mosaic of a mudstone can help reveal previously undetected micro-fabrics, textures, components and their relationships, while still preserving full-resolution detail throughout the study area. Once stitched, these mosaics are viewed in Microsoft® Research HD View, allowing the user to digitally display, zoom, and interact with the image. MAPS™ images were collected using the BSE detector. A low accelerating voltage (10kV) and a working distance of 9 mm were used.

RELATIONSHIP BETWEEN CHALK LITHOLOGY AND CHALK MICROPOROSITY

Previous work has demonstrated that contemporary permeability fields in carbonate rocks can be best described if texture (sorting and particle size) (Lucia, 1995) and pore size (Lønøy, 2006) are considered in the context of depositional and diagenetic history. In this section we integrate depositional fabric with the pore-type distribution using a modified Dunham (1962) classification that emphasizes the unique textural and depositional nature of chalk and that gives us a starting point for evaluation of diagenetic porosity modification (Figure 5).

Dunham's (1962) classification of limestone was developed with an emphasis on neritic sediments produced in what is now characterized as a *tropical carbonate factory* or *T factory* (Schlager, 2000, 2003, 2005) where carbonate mud is a common depositional component and increasing grain-to-mud ratios (mudstone to grainstone) are largely attributable to currents (tides and waves) that remove mud. Embry and Klovan (1972) expanded the textural classification scheme of Dunham (1962) to accommodate carbonate textures also common in the tropical carbonate factory, but formed by processes not discussed in detail by Dunham. These were 1) coarse-grained limestone formed in high-energy reefal and peri-reefal environments, and 2) bioconstructed framestone and biologically influenced bafflestone textures. Mei (2007) expanded Dunham's boundstone category to elucidate the genesis of textures that occur in the *microbial carbonate factory* (*M-factory* of Schlager, 2000, 2003, 2005). Herein, we propose a further expansion of Dunham scheme that focuses on the depositional processes and textural features characteristic of the ***pelagic carbonate factory***. We view this as a subtype of Schlager's (2005) T factory because sediment production is biologically controlled and sourced by tropical, photo-autotrophic organisms. However, it differs from the standard neritic T factory in that 1) grains and mud-sized particles are overwhelmingly comprised of the tests (whole, disarticulated, or broken) and fecal pellets of planktonic organisms, 2) the factory is limited in time to Late Mesozoic and Cenozoic deposits, 3) the sediment is transported vertically from the site of production by gravity, and 4) selective and/or partial dissolution of grains and mud-size particles as they descend below the lysocline has the potential to diagenetically alter sediment before

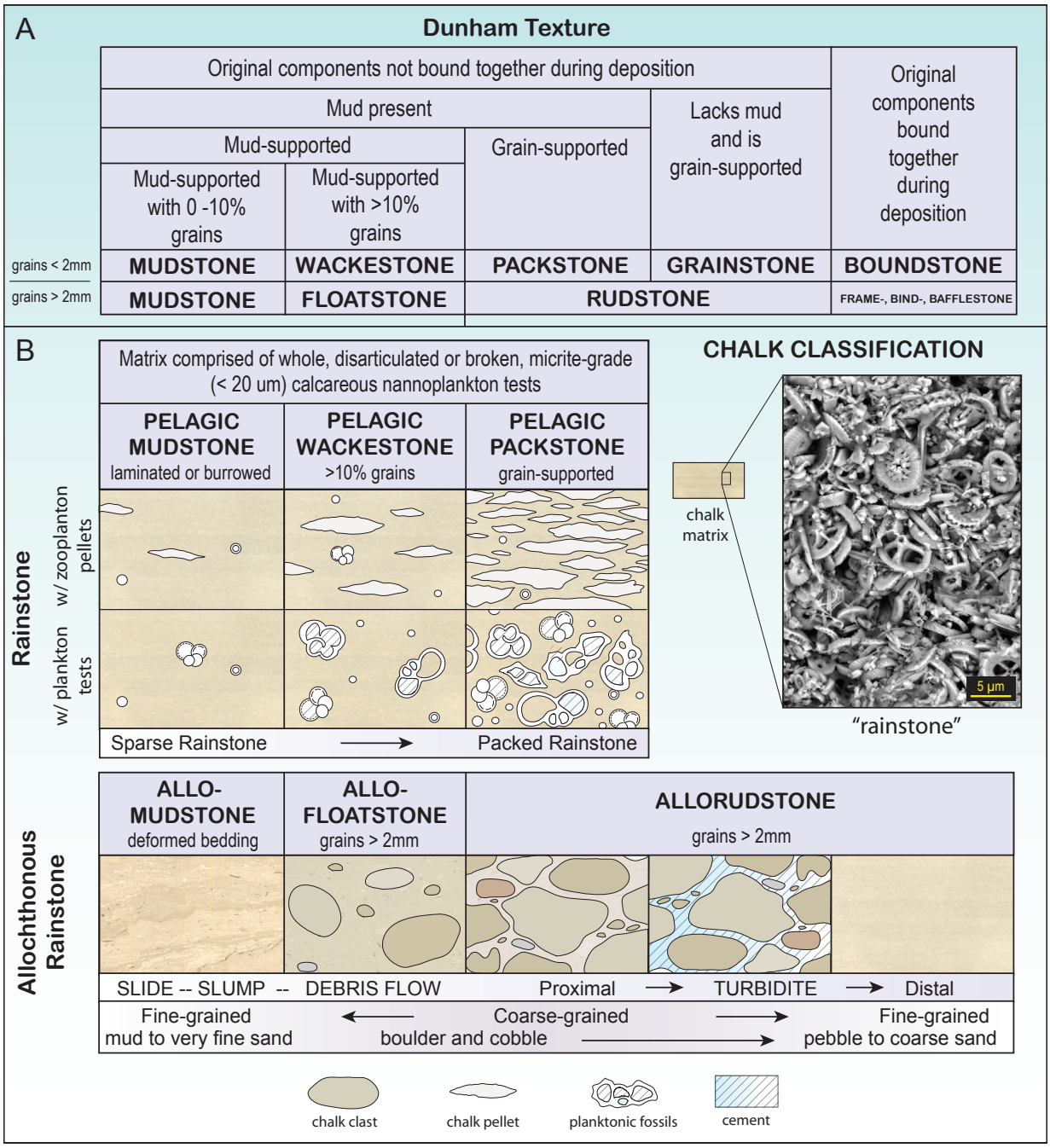

Figure 5. (A) Carbonate textural classification schemes of Dunham (1962) and Embry and Klovan (1971) compared to (B) the textural classification of pelagic and allochthonous chalk from this study.

deposition even occurs (Thierstein, 1980; Hassenkam et al., 2011). Further, textural analysis of these rocks requires specialized petrographic techniques such as discussed above.

Two categories of pelagic limestone predominate: 1) fine-grained limestone deposited

through accumulation of calcareous nannoplankton tests, fecal pellets, and aggregate particles (marine snow) on the seafloor and 2) fine- to coarse-grained limestone formed by gravity-induced, redeposition of pelagic carbonate sediments. We propose two sets of terms to classify depositional textures typical of these two categories of chalk (Figure 5). For chalk deposited by the slow "rain" of organic particles through the water column, we propose the terms pelagic mudstone, pelagic wackestone, and pelagic packstone. In keeping with the tradition of incorporating process-related terms in the names of carbonate rock types (e.g., bindstone, bafflestone, framestone), we propose the term *rainstone* for this category of pelagic chalk. For resedimented (allochthonous) chalk, we propose the terms allomudstone, allofloatstone, and allorudstone. Each of these textural subdivisions is described briefly below. We do not advocate disuse of the term chalk, but offer these terms as tools of clarification when conditions require distinction between the texture and origin of specific chalk types. The term particle is used to describe a mineral constituent of the rock. Particles less than 20 microns in diameter are called mud particles and an accumulation of such particles is termed mud (sediment) or mudstone (rock). The term grain is applied to particles greater than 20 microns in diameter.

Rainstone Textures

In this section we describe rock textures that result largely from settling of planktonic skeletal remains, fecal pellets, and marine snow (Alldredge and Silver, 1988) in the water column modified by a variety of biological, physical, and chemical processes.

Pelagic mudstone. – Chalk containing less than 10% grains. The muddy fraction is comprised chiefly of whole, disarticulated, or broken tests of calcareous nannoplankton and mud-size bioclasts of pteropods and planktonic foraminifera (Table 1). Detailed textural and compositional analysis requires electron microscopy. Mud particles range is shape from spherical (coccospheres and calcispheres) to disc-shaped (coccolith shields) to tube-shaped (coccolith tubes) to angular and blocky (individual ultrastructural crystallites). Grains (>20 microns) are comprised of pteropod and foraminifera tests, >20 micron fecal pellets (also termed chalk

Table 2. Attributes of main components of Cretaceous chalk.

TAXON	MINERALOGY	PREDEPOSITIONAL PORES	DIA. OF TEST OR SHELL	ULTRASTRUCTURE	BIOCLAST ATTRIBUTES	STYLE OF CEMENTATION
Heterococcoliths	low Mg calcite	internal cavity in coccosphere (rarely preserved intact); cavities, depressions, holes, perforations, and slits within coccoliths, cylindrical nannotubes	coccosphere = 15 to 20 µm; plates = 5 µm; central crossbars = 1 to 1.5 µm; crystalites = 0.2 to 1 µm	crystalites with a variety of simple to complex shapes that include blocks, tiles, laths, rods, wedges, petals, rays, spines, and granules: angular shape with planar crystal faces and sharp interfacial edges and corners	progressive disarticulation produces disk-shaped plates, arcuate rims and shields, bar- and cross-shaped central structures, and rhomb-, block, and lath-shaped crystalites	epitaxial cement causing increase in size of coccolith elements or fragments; increased size accompanied by retention and enhancement of blocky to rhombic shape with planar crystal facies and sharp edges and corners
Planktonic Forams	low Mg calcite	spherical to sub-spherical chambers	up to 400 µm	perforate wall structure	partially fragmented chambers or curved wall fragments	chambers partially to completely occluded by equicrystalline or drusy sparry calcite cement
Benthic Forams	low to high Mg calcite	chambers	up to 40 mm	agglutinated and porcelaneous	partially fragmented chambers or curved wall fragments	chambers partially to completely occluded by equicrystalline or drusy sparry calcite cement
Calcispheres	low Mg calcite	spherical central cavity	5 to 30 µm	NA	fragments of broken spheres	chambers partially to completely occluded by equicrystalline or drusy sparry calcite cement
Pteropods	aragonite	area bounded by shell walls, generally conical in shape	length up to 2.4 mm; with 0.5 mm	thin glassy wall	broken cones and curved planes	chambers partially to completely occluded by equicrystalline or drusy sparry calcite cement
Radiolarians	silica	area inside of test	50 to 150 µm	rods and bars	rods and bars	NA
Diatoms	silica	area within frustules	up to 15 µm	frustules	fragmented frustules	NA

pellets), and shelly benthos (e.g., bivalves, cephalopods, echinoderms). Clay and quartz silt content is less than 5%, otherwise it is termed marly pelagic mudstone (5 to 35% clay and quartz silt). Bedding, though not part of the textural definition, ranges from laminated, to partially bioturbated, to completely bioturbated and massive. Porosity ranges from 75% in modern calcareous ooze (Alam et al., 2010) to a few percent in deeply buried pelagic mudstone (Scholle 1977; Pollastro and Scholle, 1986b; Borre and Fabricius, 1998; Ings et al., 2005; Fabricius, 2007). This texture prevails in quiet water above the carbonate compensation depth. Laminated pelagic mudstone indicates a paucity of burrowing infauna due to anoxic bottom conditions. Distinct laminae are interpreted to reflect periodic (seasonal?) variation in volume and content of the pelagic rain.

Pelagic wackestone. – Mud-supported carbonate rock containing more than 10% pelagic (> 20 micron-sized forams, pteropods, calcispheres, coccospheres, and fecal pellets) and/or benthic macrofossil (oysters, echinoids, etc.) grains. Depositional processes are identical to those noted above for pelagic mudstone, but with a relatively higher contribution from grain makers such as copepods (pellets), foraminifera, pteropods, and/or shelly benthos.

The increase in grain content that distinguishes pelagic wackestone from pelagic mudstone (and packstone from wackestone) may be the result of biological processes, physical processes, or a combination of both. Biological processes that control the ratio of mud- to grain-making plankton in the near-surface environment (and in undistorted bottom sediment) include seasonal controls on productivity and differences in species-specific productivity. Physical phenomena that distort the composition and size (mud particles versus grains) of bottom sediment include disarticulation and fragmentation of tests, grazing and packaging of tests in fecal pellets, selective or bulk dissolution of particles in the water column, and lateral advection of particles by currents. Mixing (time averaging) of young and older sediment should be assumed where primary lamination is disrupted or obliterated by burrowing. "Currents of removal" (sensu Dunham), the chief determinant of sedimentary texture in neritic limestone (sensu Dunham), play only a minor role in the pelagic realm. The meaning of a specific wackestone (or packstone) may be difficult to interpret given that a range of oceanic processes have operated selectively or pervasively on the plankton-rich sediment from the instant of production to the time of deposition. Post-depositional compaction (physical and chemical), dissolution, cementation, and neomorphism may further modify the texture (Scholle, 1977)

Pelagic wackestone is best characterized using electron microscopy; however, the contrast between mud matrix and grains can be ascertained using normal thin-section petrographic techniques. Clay and quartz silt content is less than 5%, otherwise it is termed marly pelagic wackestone. Bedding ranges from laminated, to partially bioturbated, to completely bioturbated (massive).

Pelagic packstone. – Grain-supported, mud-bearing chalk resulting from abundance of grains relative to mud-size particle contributors. Grains may be predominantly chalk pellets, (copepod pellets) such as is common in the Smoky Hill Member of the Niobrara or tests and shells of larger planktonic or benthonic organisms. This texture may result from any of the biological, physical, and/or early diagenetic processes (mentioned above) that control the mud-to-grain ratio in seafloor sediment. Clay and quartz silt content is less than 5%, otherwise it is

termed marly pelagic packstone. Bedding may range from laminated, to partially bioturbated, to completely bioturbated and massive.

Pelagic grainstone textures resulting from settling of planktonic sediments in the water column are rarely encountered in chalks. This is because most voids between grains are filled with mud-sized particles.

Allochthonous Chalk Textures

In this section we describe textures that result from syndepositional tectonic disruption of the seafloor resulting in mass-movement of chalk at scales that vary from decimeter-thick turbidites to slide sheets up to several hundred meters in thickness (Watts et al., 1980; Hatton, 1986; Herrington et al., 1991; Van der Molen et al., 2005; Ineson et al., 2006). This includes those textures formed from soft-sediment deformation, seismites and other minor mass-movement features. With respect to porosity, a relationship between redeposited textures and higher porosities has been suggested by several researchers (Hardman, 1982; Hatton, 1986; Kennedy, 1987; Anderskouv and Surlyk, 2012).

Allomudstone. – Identical to pelagic mudstone at the scale of thin-section and SEM photomicrographs. At core and outcrop scale, this texture is indicated by contorted bedding resulting from cohesive transport of partially lithified chalk or subtle color banding resulting from interbedding of rainstone with low-density turbidites and fall-out clouds of resuspended material. Mudflow deposits may result in formation of structureless chalks (Aderskouv and Surlyck, 2011). As a general rule, we assume muddy chalk to be of pelagic origin (rather than allochthonous mudstone) unless there exists clear evidence of syndepositional disruption in the form of graded beds, glide planes, soft-sediment deformation, and/or chalk-clast floatstone, etc. in associated beds.

Allofloatstone. – Mud-supported carbonate rocks containing more than 10% large (> 2mm) randomly distributed clasts of chalk, lithics, and bioclasts. Lithic clasts are comprised of non-carbonate (clay, quartz silt) sediments of pelagic origin (Aderskouv and Surlyck, 2011).

Chalk clasts range in size from pebbles to boulders, are rounded to subangular in shape, and lack any preferred orientation. The matrix is usually structureless and may be more porous than the clasts (Anderskouv and Surlyck, 2012). The presence of large clasts "floating" in a structureless matrix indicates lithification of a viscous debris flow (Lowe, 1982).

Allorudstone. – Clast-supported carbonate rocks with variable amounts of interstitial mud. Chalk clasts predominate in matrix-rich rudstone. Matrix-rich rudstone is similar to debris flow floatstone described above and may be deposited by the same mechanism, but may also represent deposition by proximal turbidites. Matrix-poor rudstone typically displays graded or inverse-graded bedding suggesting deposition by down-slope maturation of turbidite flows whereby mud was expelled from the flow (Anderskouv and Surlyck, 2011). Chalk clasts predominate with variable amounts of shell debris. Clasts range in size from cobble to coarse sand depending upon distance from source. Units with this texture have sharp and loaded bases (Anderskouv and Surlyck, 2011, 2012). For a more complete discussion of carbonate gravity flow processes and deposits we refer the interested reader to Lowe (1982), Hatton (1986), Flugel (2004), and Anderskouv and Surlyck (2011, 2012).

CLASSIFICATION OF CRETACEOUS CHALK MICROPORES

One of the essential differences between Lønøy's (2006) carbonate pore-type classification and those that preceded it (Choquette and Pray, 1970; Lucia, 1983, 1995, 1999) was the introduction of a new category for Cretaceous and Tertiary chalk that he named mudstone microporosity. Other than the small size (< 10 microns) and the suggestion that micropores occur between grains of planktonic coccoliths, Lønøy (2006) elaborated very little on the nature, origin, and evolution of mudstone microporosity. Prompted by increasing interest in carbonate resource plays, we provide a description of the variety, shape, size, and origin of carbonate mudstone microporosity based upon a study of the Niobrara "B" chalk and marl from the Denver-Julesburg (DJ) Basin in Colorado, Wyoming, and Kansas.

Based upon our study of the Niobrara Formation, we find that chalk micropores differ

from pore types observed in conventional carbonate reservoirs in four critical ways: 1) they display only a limited number of the primary pore types described by Choquette and Pray (1970), 2) the pores are much smaller in size, 3) they are modified by a relatively small range of possible diagenetic processes, and 4) organic matter-hosted pores that form during hydrocarbon generation are much more common (Jarvie et al., 2007; Loucks et al., 2009; Slatt and O'Brien, 2011; Loucks et al., 2012).

Recent efforts at describing and classifying pore types in mudstones have been made by Slatt and O'Brien (2011) and Loucks et al. (2012). These studies have focused primarily on siliceous, gas-producing unconventional reservoirs and have, with few exceptions, completely ignored calcareous, mixed oil-and-gas producing unconventional reservoirs. What follows is a description of four basic pore types and ten subtypes that commonly occur in the Niobrara Formation (Figure 6) and that collectively constitute the Cretaceous chalk micropore subclass of Lønøy (2006). In this section we describe the origin, size, and distribution of these pore types, saving a discussion on diagenesis for a later portion of the paper.

Interparticle Pores

We follow Choquette and Pray (1970) in defining interparticle porosity as porosity occurring between mineral particles of any size. In chalk, two dominant families of depositional particles are distinguished based upon their size and origin: small particles comprised of distarticulated and fragmented remains of planktonic algae and larger particles comprised of foraminifera and pteropods tests, macroinvertebrate shells, and fecal pellets. The former particles, which are generally less than 20 microns in diameter are herein called *mud* or *micrite particles.* Particles greater than 20 microns are called *grains*. The term *platelet* is used to describe phyllosilicate crystallites regardless of size. Four types of interparticle pores are common in the Smoky Hill Member (Figures 7 and 8).

Interskeletal. – Interskeletal porosity is the dominant type of porosity in clean rainstone of the Niobrara Formation (Figure 7A). In shallowly buried chalk, skeletal particles are

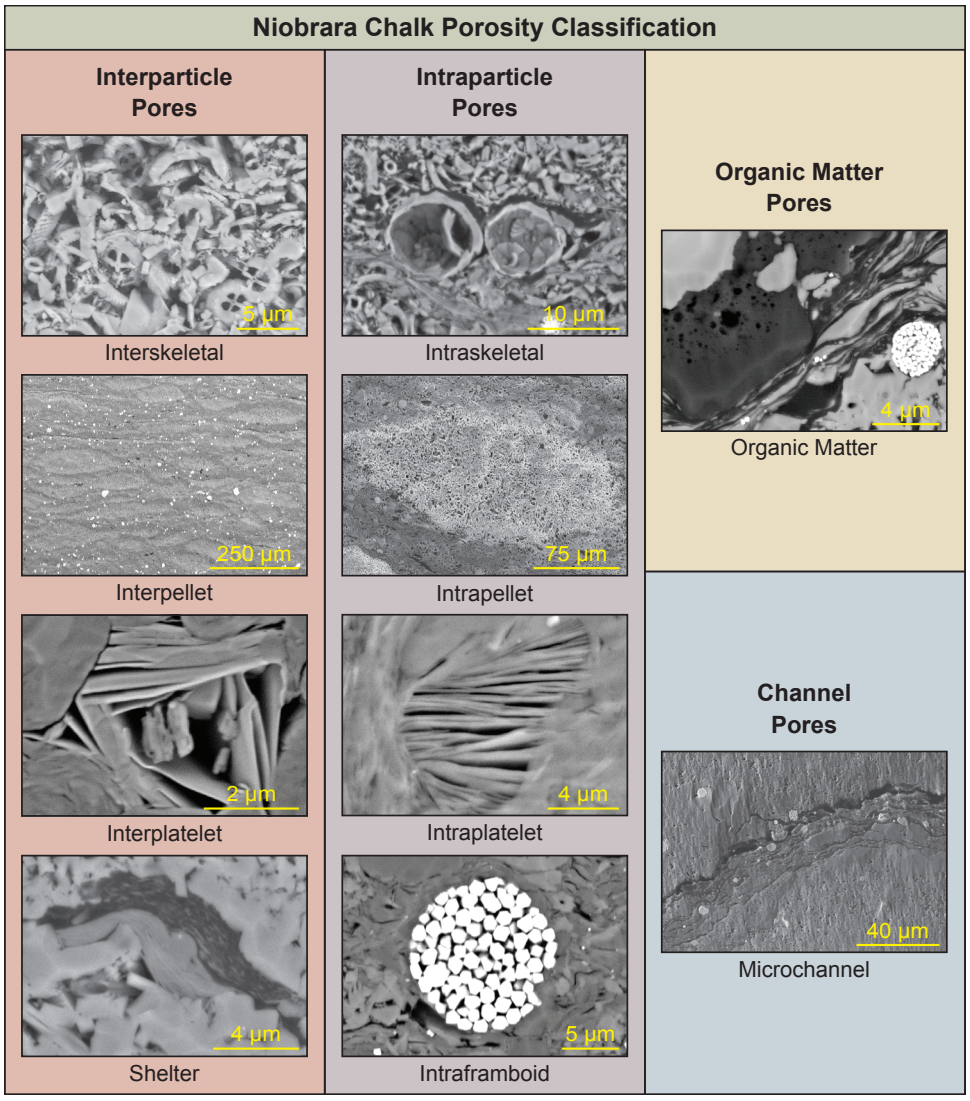

Figure 6. Scanning electron photomicrograph (SEM) spectrum of pore types occurring within the Niobrara Formation. General porosity class types include interparticle and intraparticle, under which further subtypes are presented, as well as organic matter and channel.

comprised of 1) small, disarticulated, and fragmented coccoliths that range in size from 2 to 20 microns in diameter and 2) larger particles comprised of foraminifera and pteropods tests, calcispheres and macroinvertebrate shells. Pore geometry is determined by the shape of the constituent particles. In small skeletal particles these are discoidal (coccolith plates), arc-shaped (coccolith plate fragments), blocky (individual coccolith crystallites), and cylindrical (coccolith tubes). Most pores have diameters in the low micrometer range but can range anywhere from 100 nm to 10s of microns. In shallowly buried pelagic mudstone, pore abundance, measured in SEM

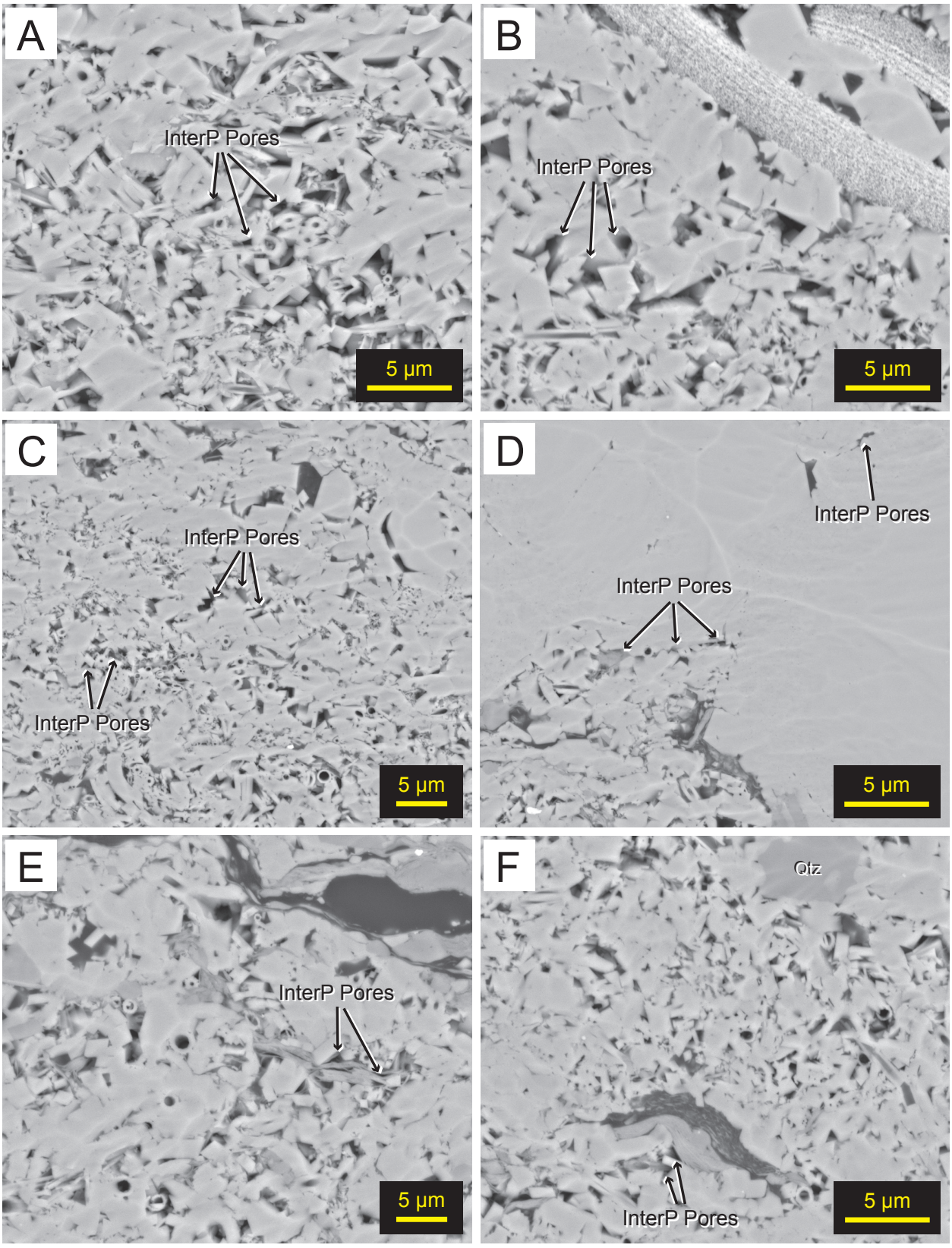

Figure 7. SEM photomicrograph examples of interparticle (InterP) pores from an Ar-ion milled Niobrara chalk core sample (Well: Burbach 20-3H; Depth 7193.5 ft. (2192.6 m)). (A) Interskeletal pores between coccolith fragments. (B) Interskeletal pores between calcite cement overgrowths. Pores have jagged, triangular outlines. (C) Interparticle pores in a typical chalk matrix consist of a mixture of pores between whole coccoliths, coccolith fragments, tubes and calcite cement overgrowths. (D) Interparticle pores between the coccolith-rich matrix and a foram test. (E) Linear interplatelet pores between clay floccules. Pores between floccules are rare in chalk samples because clays are not very abundant. (F) Shelter pores preserved under a deformed clay grain and organic matter 'lake'.

photomicrographs by 1200 point counts of ion-milled samples, ranges from 27 to 38%.

Where more deeply buried, breakage and syntaxial overgrowths render the majority of coccolith fragments equant and blocky with a concomitant change in pore geometry and overall reduction in pore size (Figures 7B, 7C, and 8A-C). Measured porosity by point count is reduced to a range of 5 to 17%.

Interpellet. – Interpellet porosity is defined as pores between chalk pellets. Conceptually, this type of porosity would reach maximum abundance in uncompacted, washed pelagic packstone or pelagic grainstone but as mentioned previously, pelagic grainstone textures are rarely, if ever, encountered in the Smoky Hill or, for that matter, in other chalks. Most areas between grains are filled with mud-size particles. Hence, interpellet porosity is volumetrically unimportant in most chalks. Increasing amounts of clay occupy the interstices between grains in chalky marl and marl lithologies (Figures 7D and 8D).

Interplatelet. – Interplatelet pores are primary pores that have been preserved between individual clay platelets (Figures 7E and 8E). These pores are typically elongate and may be parallel to one another in cross section. Interplatelet pores are not common in clean Niobrara chalk lithologies, but increase in abundance as chalk-rich transitions to chalky marl and marl.

Shelter. – Shelter pores are created by the sheltering effects of rigid grains or where more ductile grains bend around more rigid grains (Choquette and Pray, 1970; Loucks et al., 2012). This sheltering prevents the filling of pore space by finer sedimentary particles. In the Niobrara, both rigid and ductile grains have been observed (Figures 7F and 8F) to create shelter pores and these are present throughout the chalk to chalky marl to marl transition.

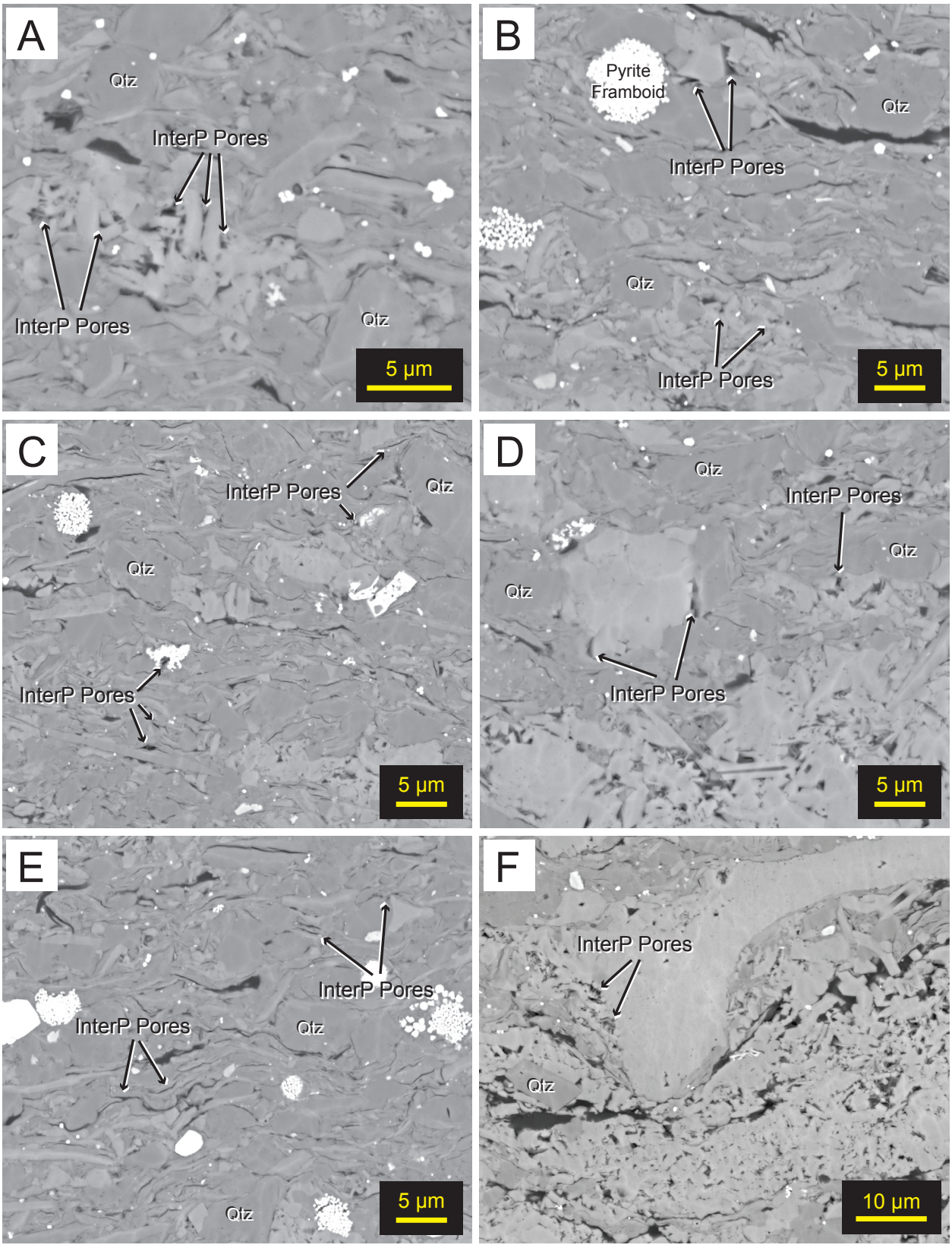

Figure 8. SEM photomicrograph examples of interparticle (InterP) pores from an Ar-ion milled Niobrara marl core sample (Well: Lee 41-5; Depth 7986.5 ft. (2434.3 m)). (A) Interskeletal pores between coccolith fragments and calcite cement overgrowths in a marl matrix. (B) Interparticle pores between coccolith fragments, quartz silt and clay grains. (C) Interparticle pores between grains and coccolith fragments. (D) Interparticle pores preserved around the edges of a carbonate grain. (E) Linear interparticle pores between clay floccules. (F) Shelter pores preserved adjacent to a large carbonate grain that has deformed a chalk fecal pellet.

Intraparticle Pores

Intraparticle pores are those occurring within particles (Figures 9 and 10). In chalk, most of these pores are primary and predepositional in origin. As phyllosilicate content increases, so does the content of cleavage-plane pores within marly chalk and chalky marl. Intercrystalline pores within diagenetic pyrite framboids are included in this category. Each of these categories is described below.

Intraskeletal. – Pre-depositional micropores that form within skeletal particles of coccospheres, coccoliths, nannotubes, foraminifera and pteropods tests, calcispheres and macroinvertebrate shells (Figures 9B, 9C and 10B). Coccolith related pores range in size from less than 1 to 15 microns in diameter and in shape from spherical (center of whole coccospheres and foram tests) to oval (center of coccolith shields) to cylindrical and elongate (interior of coccolith tubes). Intraskeletal pores within foraminifera and other skeletal particles are larger and assume the shape and size of the confining shell wall (Figures 9D, 10D and 10E). Intraforaminiferal pores are typically spherical in shape and range in size from 10 to 40 microns. In pelagic wackestone, intraforaminiferal pores are isolated or non-touching so contribute little to the permeability of the rock. Even where foraminifera are highly concentrated in pelagic packstone, skeletal walls restrict permeability. Additionally, in most instances, individual chambers are filled with equant sparry calcite cement or pyrite crystals. In both shallowly and deeply buried rainstone, these comprise less than 1% of the rock volume as observed by point count.

Intrapellet. – Intrapellet porosity consists of pre-depositional pores found within chalk fecal pellets. In chalks and chalky marls of the Smoky Hill Member, fecal pellets are the most

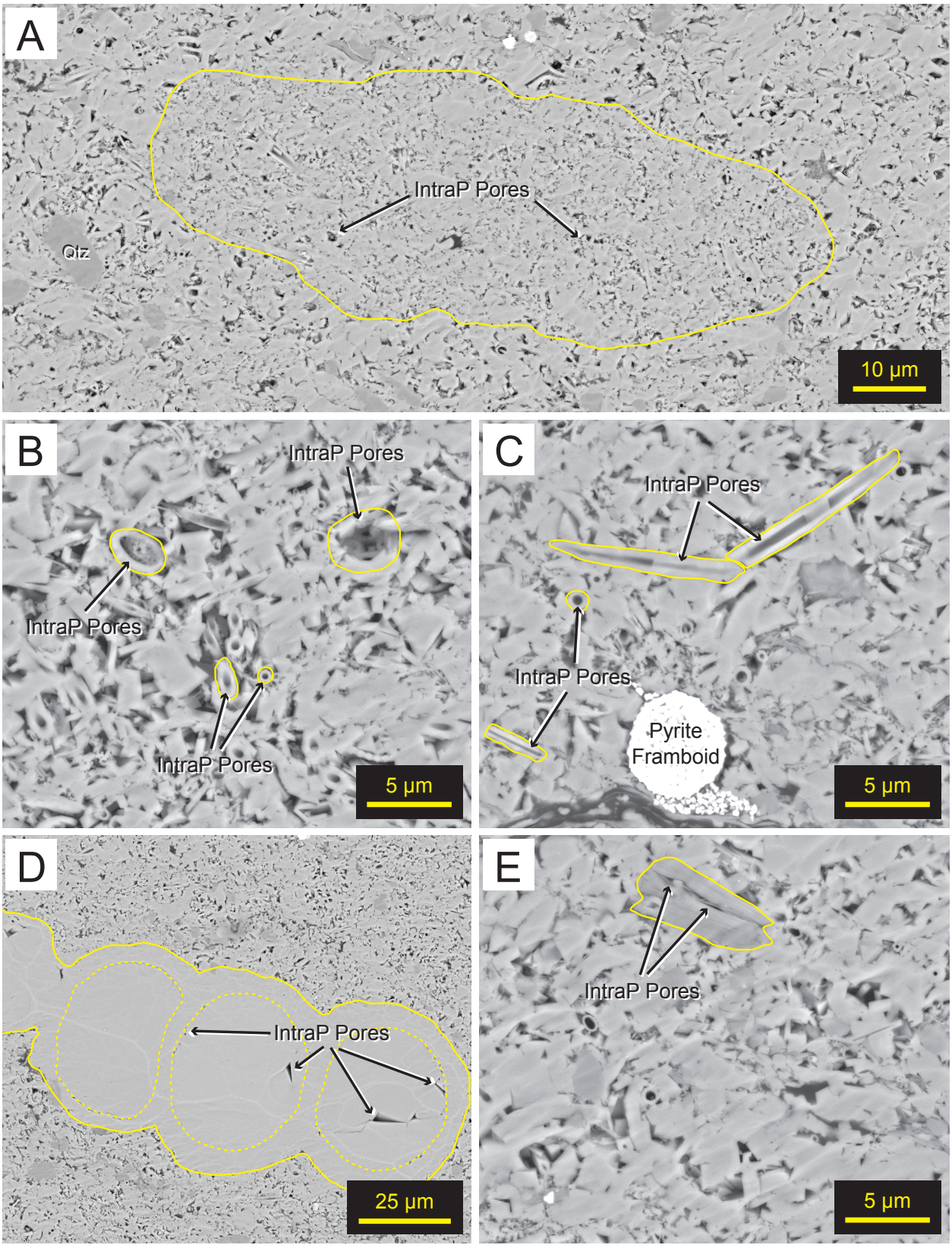

Figure 9. SEM photomicrograph examples of intraparticle (IntraP) pores from an Ar-ion milled Niobrara chalk core sample (Well: Burbach 20-3H; Depth 7193.5 ft. (2192.6 m)). (A) Intrapellet pores are most common as pores in coccolith-rich fecal pellets. Porosity within pellets consists of interparticle and intraparticle pores between and in whole coccoliths, coccolith fragments, tubes and calcite cement overgrowths. (B) Typical intraparticle pores in a chalk matrix consist of pores within whole coccoliths, tubes and an occasional undisarticulated coccosphere. (C) Intraparticle pores within coccolith tubes differ in size (length and width), orientation and dimension. (D) Cement reduced intraskeletal pores resulting from cementation of a hollow foram test. (E) Linear intraparticle pores within a clay floccule.

common particle type, producing a conspicuous speckling in hand sample and core. These range in size from 100 to 250 microns. In vertical section, pellets have elliptical cross sections that become more elongated and irregular with increasing burial (Figures 9A and 10A). In the plane of stratification, the compacted pellets are circular to elliptical in shape. Pores within chalk pellets are identical in shape and distribution to interskeletal pores between small, disarticulated, and fragmented coccoliths described previously, only they occur within the confines of pellets. In pellet-rich pelagic packstone and in physically compacted pellet-rich chalk, individual pellets touch each other and are surrounded by pelagic muds, making the rock a *de facto* pelagic mudstone with respect to porosity and permeability. In chalky marl and marl, the pellets become increasingly isolated domains of intraparticle porosity surrounded by clay.

Intraplatelet. – Intraplatelet pores are pores found within individual clay platelets and are related to either clay cleavage planes or are residual pore spaces within clay flocculates (Figures 9E and 10C). They are typically elongate and parallel to one another in cross section. Like interplatelet pores, they are not as common in chalk as they are in chalky marl and marl lithologies.

Intraframboid – These are intercrystalline pores within pyrite framboids (Loucks et al., 2012; Figures 9C and 10A). Framboids range from a few to 10 microns in size. Pores range in size from 0.2 to 0.8 microns. Pore shape is controlled by the shape and arrangement of the crystals comprising the framboid. Many of these pores are occluded with organic matter that may contain organic matter pores. They are diagenetic or secondary in origin and contribute very little to the permeability of typical chalks and marls.

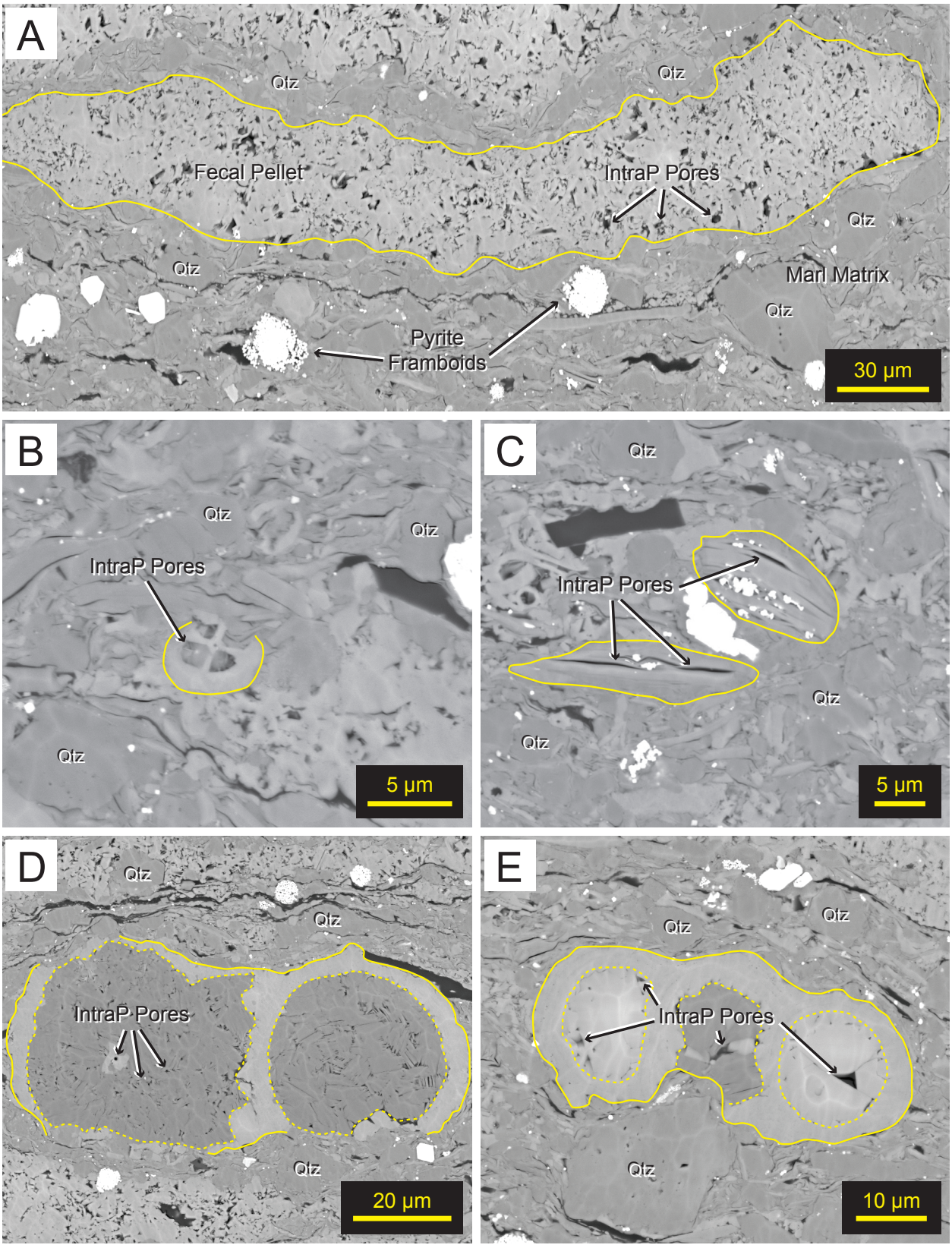

Figure 10. SEM photomicrograph examples of intraparticle (IntraP) pores from an Ar-ion milled Niobrara marl core sample (Well: Lee 41-5; Depth 7986.5 ft. (2434.3 m)). (A) Intrapellet pores are most common as pores in coccolith-rich fecal pellets. Pores within pellets consist of interparticle and intraparticle pores. Marl intraparticle pores differ from those in chalk litholigies as most are filled with organic matter and contain organic matter (OM) pores. (B) Intraparticle pores within a coccolith preserved in the matrix. (C) Linear intraparticle pores within clay floccules. (D) Intraparticle pores between clays within foram test chambers. (E) Cement reduced intraskeletal pores resulting from cementation of a hollow foram test.

Organic Matter Pores

Organic matter pores are related to burial and thermal maturation of organic matter and occur as a result of hydrocarbon generation (Loucks et al., 2009; Figures 11 and 12). These pores have been described as irregular, bubble-like, pendular, spongy, elliptical and fracture or crack based (Loucks et al., 2012; Driskill et al., 2013; Milliken et al., 2013). They generally range in size between 5 and 750 nm in length (Loucks et al., 2012); however, during this study, organic matter pores were found to be several microns in cross section (Figures 11C and 11D). Though they do exist in chalk lithologies, organic matter pores are most common in chalky marl and marl lithologies where organic matter is more abundant.

Organic matter pores in the Niobrara Formation are principally found in organic matter residing within interparticle pores within chalk fecal pellets (organic matter pores in interparticle pores in intraparticle pores; Figures 11A and 12A). It is still unclear how organic matter comes to reside within pores in chalk pellets. One might expect some organic matter would accompany copepod excrement. If not depositional, then it may be related to compaction and diagenesis, the organic matter being squashed in-to the pellets during compaction. It is also possible they are pores in dried out, residual hydrocarbons. Organic matter pores are also found within individual organic matter lakes (Figures 11C, 12C and 12D) and within the concentrated organic matter of a microstylolite (Figures 11B, 12E and 12F).

Microchannel Pores

Channels are an important part of a carbonate porosity classification. Where present, they can have significant influence on hydrocarbon production, providing additional storage and more

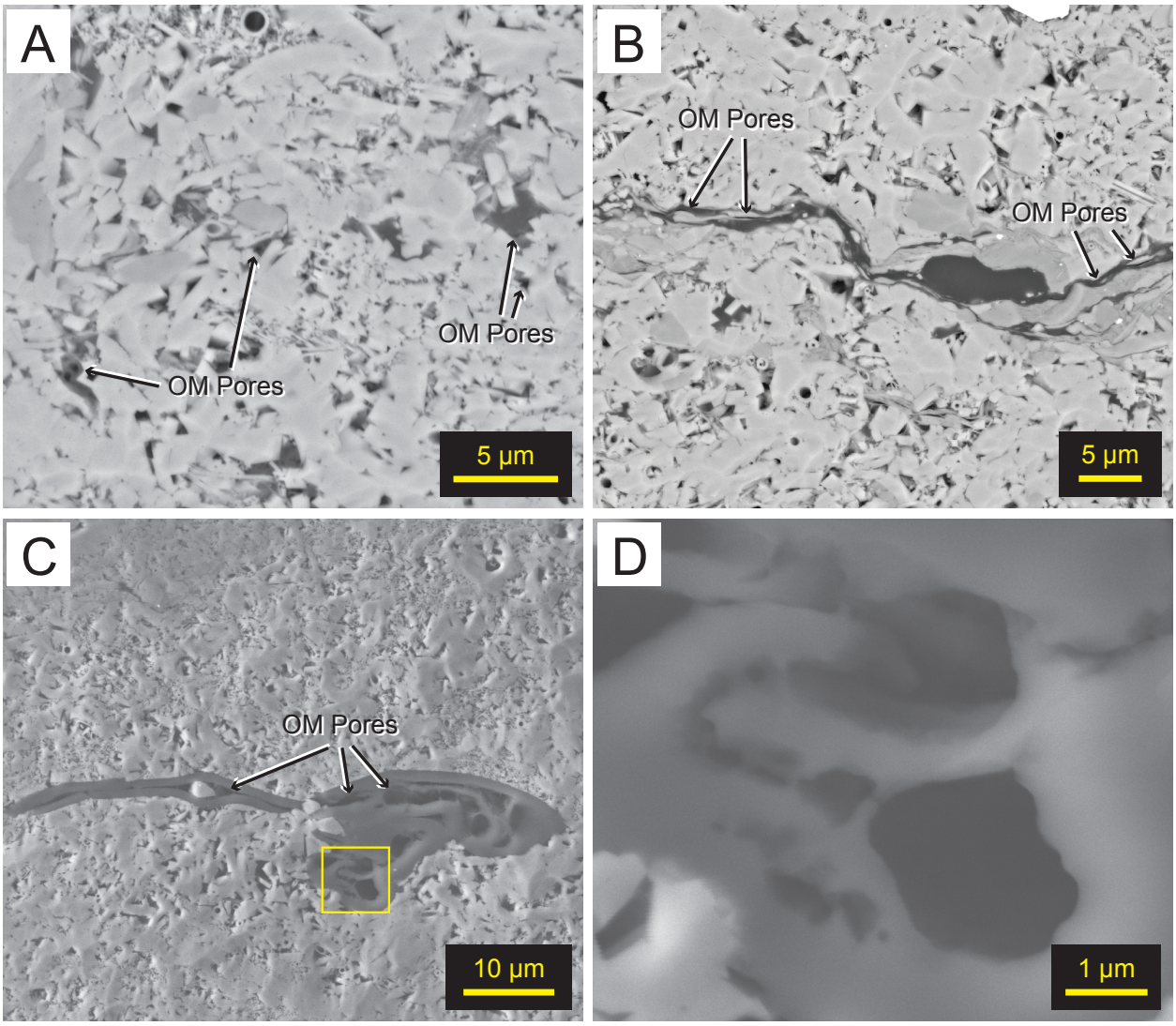

Figure 11. SEM photomicrograph examples of organic matter-related (OM) pores from an Ar-ion milled Niobrara chalk core sample (Well: Burbach 20-3H; Depth 7193.5 ft. (2192.6 m)). (A) OM pores occurring in organic matter found between matrix coccolith fragements, tubes and calcite cement overgrowths. Pores vary in size and display ellipsoidal shapes. (B) OM pores occurring in the concentrated organic matter of a microstylolite. Pores are elongate in the same orientation as the microstylolite and are usually associated with mineral particles. (C) Large OM pores in an isolated organic matter 'lake' in a micrite matrix. Pores display slight alignment and complexity in the third dimension. Box shows view area of (D). (D) High magnification zoom in of OM pores showing extra detail of large pores (>1 µm) displaying a bubble-like texture.

effective permeability pathways (Slatt and O'Brien, 2011). Choquette and Pray (1970) suggested 'channel' be used for elongate pores or irregular openings with obvious elongation or continuity in one or two dimensions relative to a third. They also labeled channel pores less than 1/16 mm in cross section or thickness as 'microchannels'. We use the term microchannel to describe

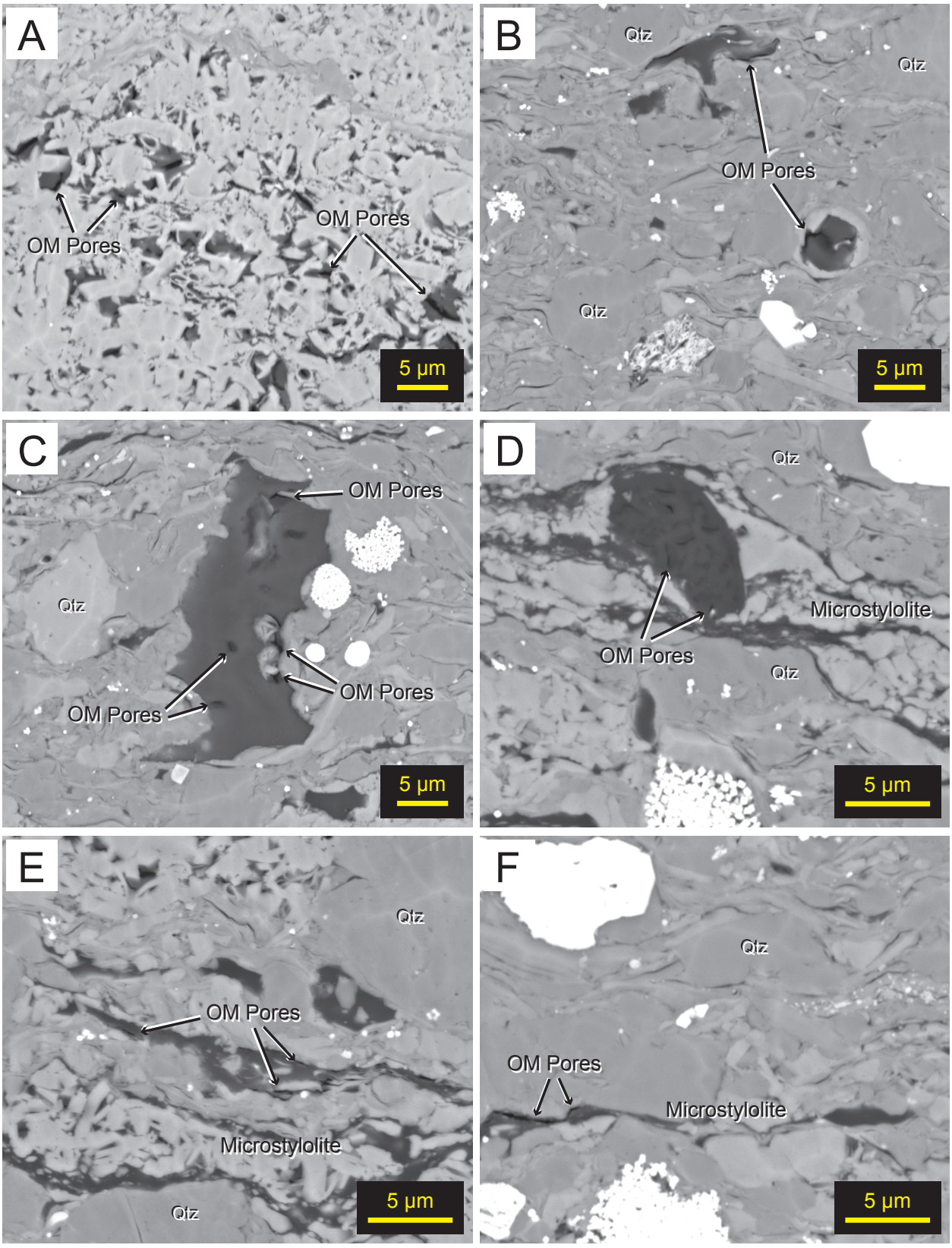

Figure 12. SEM photomicrograph examples of organic matter-related (OM) pores from an Ar-ion milled Niobrara marl core sample (Well: Lee 41-5; Depth 7986.5 ft. (2434.3 m)). (A) OM pores are most abundant in OM-filled interparticle and intraparticle pores within coccolith-rich fecal pellets. The size and shape of pores varies based on the amount of OM present. Most occur as elongated ellipses and cracks. (B) OM pores observed in the matrix occur within OM 'lakes' and individual OM filled fossil fragments. (C) Large isolated OM 'lake' containing small elliptical and crack shaped pores. (D) OM 'lake' in a microstylolite containing very small crack shaped pores. (E) and (F) OM pores occurring in the concentrated OM of a microstylolite.

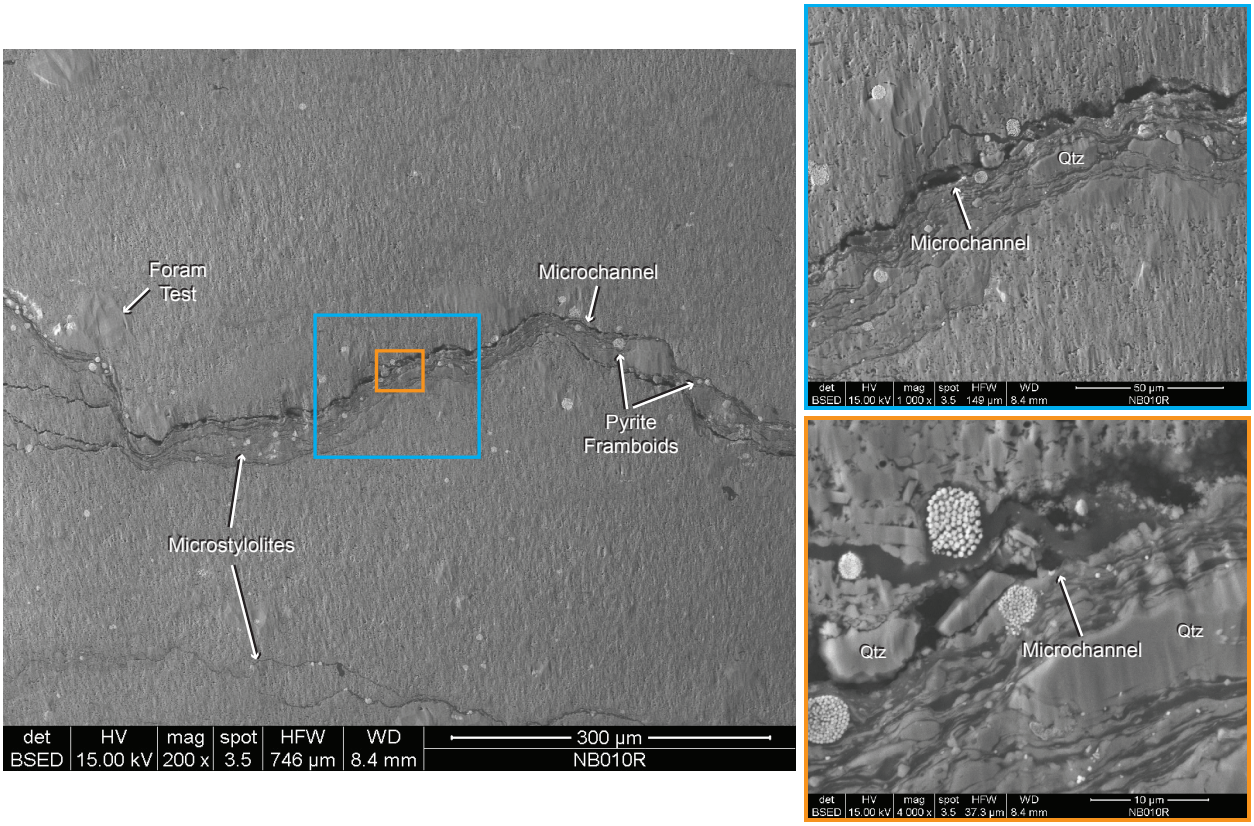

Figure 13. Successive zoom-in SEM photomicrograph views of microchannel pores found within a microstylolite from an Ar-ion milled Niobrara chalk core sample (Well: Burbach 20-3H; Depth 7193.5 ft. (2192.6 m)). The large low magnification (200x) image shows a chalk matrix with multiple microstylolites consisting of partially dissolved carbonate grains, quartz silt, clays, and pyrite in and around concentrated organic matter. Colored boxes show areas of the medium (1,000x) and high (4,000x) magnification photomicrographs on the right.

features in the Niobrara that fit this definition.

Microchannels of various size and shape have been observed during UV-light thin section and SEM analyses of Niobrara Formation samples (Figure 13). They occur within microstylolites

consisting of concentrated partially dissolved carbonate foram tests and coccolith-rich fecal pellets, and insoluble residues (quartz silt, clays, pyrite, and other heavy minerals) in and around an organic matter matrix (Figure 14). Like microstylolites, Niobrara microchannels are sinuous and discontinuous and form subparallel to bedding planes. Their length varies based on the length of the microstylolite in which they form. Those observed in this study extend hundreds of microns to only a few tens of centimeters until bifurcating and fading into the matrix. Observed microchannels are present in chalk, chalky marl, and marl lithologies and are less than 1 to 5 microns in width.

There are two possible explanations for the formation of microchannels in the Niobrara Formation. The first is simple and pertains directly to the development of organic matter pores within concentrated organic matter found in a microstylolite. If enough organic matter pores are created they may eventually link together and form a horizontal channel. More complicated, the second is similar to creation of a bedding-parallel fibrous calcite 'Beef' in shale and is believed to be a function of overpressure created by mechanical compaction, hydrocarbon generation or a combination of both (Cobbold et al., 2013). To produce horizontal channels, overpressure must exceed the overburden pressure, causing the vertical effective stress to become tensile and the rock to eventually fail in tension (Cobbold et al., 2013). For this to work, it is assumed that concentrated organic matter within a microstylolite has a weaker crystal lattice than that of the surrounding rock matrix, acting as a plane of weakness where microchannels can form. Of course it is entirely possible and highly likely that these two processes occur in tandem, overpressure linking individual organic matter pores as the Niobrara enters the thermal maturity window.

Distinguishable in multiple samples, we suspect microchannels in the Niobrara Formation exist in abundance where lithology and thermal maturity come together in the right proportions. Evidence in support of this suspicion can be found in cores recovered in areas where the Niobrara is not overly calcareous or argillaceous and in the thermally mature window (i.e., Wattenberg Field). These consistently break and fall apart along microstylolites.

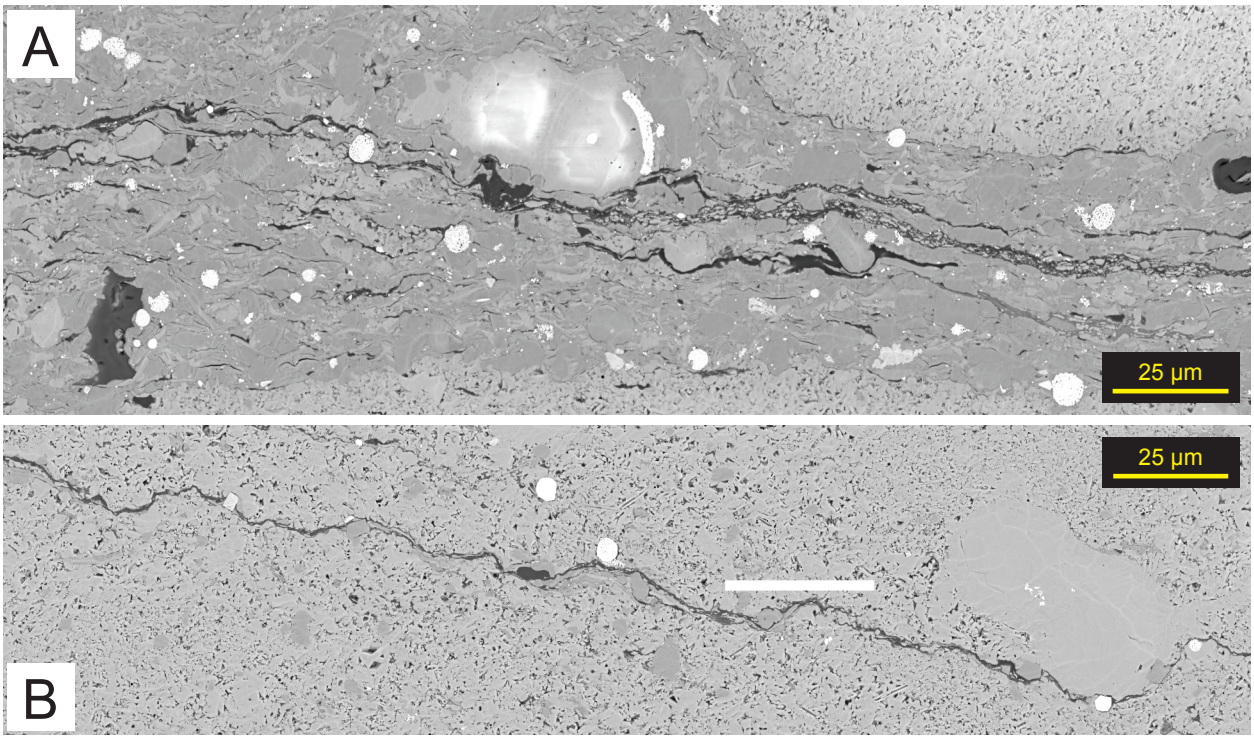

Figure 14. Stitched SEM photomicrograph examples of Niobrara Formation microstylolites (Well: Burbach 20-3H; Depth 7193.5 ft. (2192.6 m)). (A) Marl microstylolite with concentrated organic matter, quartz silt, clays and pyrite as well as partially dissolved carbonate grains (foram test in upper center). (B) Smaller chalk microstylolite consisting of the same undissolved constituents (partially dissolved foram test right center). The white rectangle is a gap in the photomicrograph data set.

Fracture Pores

Facture-related pores are not part of the Niobrara Chalk Porosity Classification presented here (Figure 6) because there were no open fractures imaged during this study; nevertheless, we recognize the presence of fracture pores in the Niobrara Formation and that they can have a significant effect on hydrocarbon production. Niobrara fractures be created in a number of ways and occur at a variety of scales (Sonnenberg, 2011b). Wyoming's Silo Field, located in the northern part of the DJ Basin, is an excellent example of production from fractures in the Niobrara (Sonnenberg, 2011a)

Comparison

It is important to identify the abundance and distribution of pore types within mudstones

since each contributes differently to permeability and thus, reservoir producibility. Because of similar constituents (i.e., chalk pellets), Niobrara lithologies contain similar pore types; however, the abundance of those constituents will greatly affect the connectivity of the pore network. In order to more fully understand pore connectivity and communication, proportions of pore types within Niobrara chalk and marl lithologies are presented on the ternary diagram in Figure 15.

Within both chalk and marl lithologies, pore type is strongly influenced by the relative abundance of flattened chalk pellets. These pellets are most abundant in chalk lithologies except where they are massively bedded and heavily bioturbated (Longman et al., 1998). Similarly, chalk pellets can make up a significant portion of marl lithologies where extensive bioturbation has not occurred. Hence, where chalk pellets are abundant, both lithologies exhibit a strong intraparticle pore network; however, as the abundance of chalk pellets decreases, so does the intraparticle influence. In pelagic mudstone where few chalk pellets are present, both lithologies

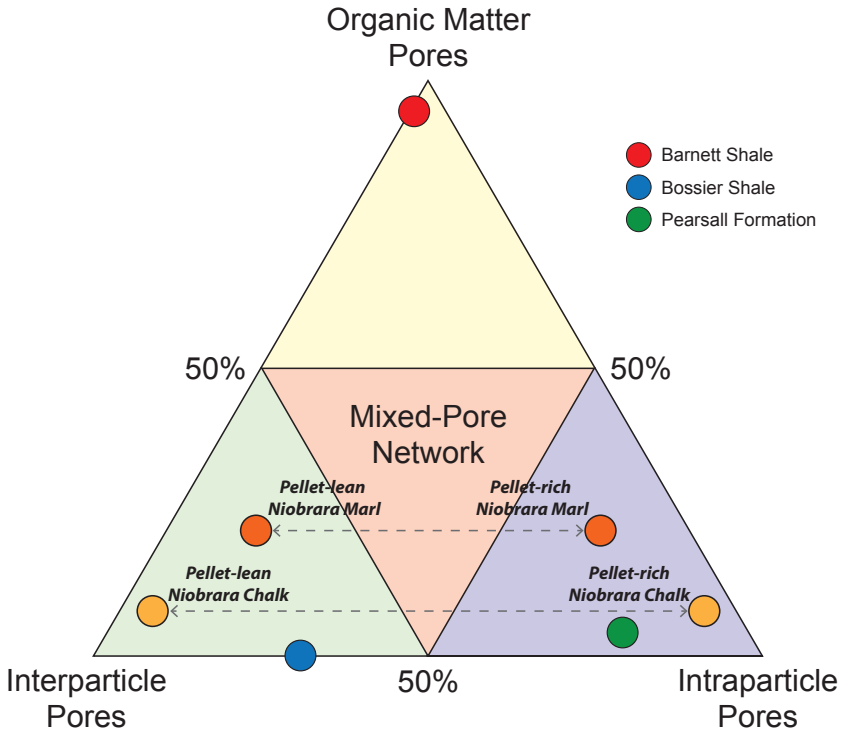

Figure 15. Mudrock pore classification ternary diagram modified from Loucks et al. (2012) with examples of pore networks from the Barnett Shale, Boosier Shale, and Pearsall Formation. The proportion of pore types for Niobrara chalk and marl are based upon careful visual assessment. Data placement is strongly influenced by the relative abundance of chalk fecal pellets within a given sample.

display a strong interparticle pore network. This variability is demonstrated in Figure 15 as a sliding scale between interparticle and intraparticle pore networks and with distinction between pellet-lean and pellet-rich.

CHALK TO MARL TRANSITION

Despite the widely held notion that the Smoky Hill Member of the Niobrara Formation consists of relatively uniform chalk and marl sequences, lithologies and thus pore networks vary considerably, both laterally and vertically across the DJ Basin between chalk, chalky marl, and marl. This variation is largely a function of changes in the abundance of flattened chalk pellets relative to matrix micrite and clays (Longman et al., 1998). As noted previously, primary constituents of the Niobrara include flattened chalk pellets, planktonic foram tests, oyster and inoceramid shell fragments, micrite-grade coccolith and coccolith fragments, clays, quartz silt, pyrite, and organic matter. As such, these rocks can be classified based on the relative abundance of carbonate and siliciclastic components. To aid us in lithologic classification, study samples were observed in thin section and QEMSCAN® analyses were performed. Our classification (Figure 16) is modified from Longman et al. (1998).

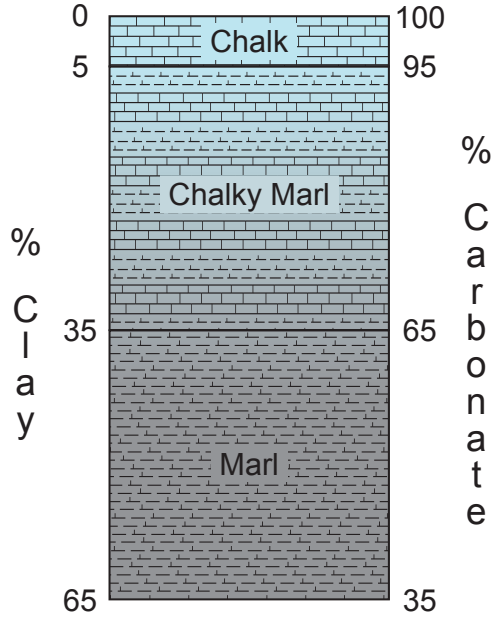

Figure 16. Niobrara Formation chalk to marl spectrum modified from Longman et al. (1998).

There is generally little megascopic variation in appearance between these lithologic types besides color. The more clay-rich lithologies are commonly darker while the amount of organic matter may also affect color. Where present, flattened chalk pellets impart a white speckled appearance that is evident in the majority of Niobrara samples. The following discussion provides a general lithologic description of each of the three main Niobrara lithologies.

Chalk

Niobrara chalk deposition in the Western Interior Basin was strongly influenced by warm waters from the Gulf of Mexico (Sonnenberg, 2011b). These waters brought with them a rich carbonate flora of coccoliths and promoted carbonate production and deposition. In the DJ Basin, Niobrara chalks are light- or olive-grey and can be laminated or massive. Bedding structures include parallel, wispy and slightly burrowed laminae. Chalks are richest in flattened chalk pellets. Pellets make up 65 to 90% of the rock, except where they have been destroyed by bioturbation (Longman et al., 1998; Figure 17). The matrix is dominated by micrite-grade skeletal particles with little silt or clay. Foram tests are moderate to abundant and are filled with calcite cement and pyrite. Oyster and inoceramid shell fragments are common locally. Pyrite framboids are rare and are usually associated with silts and clays. Microstylolites are rare to moderate and contain organic matter and undissolved solids. Dissolution features can be difficult to discern but are present. Organic matter is also rare. It occurs primarily as visible organic matter 'lakes' and occasionally within pellets between coccolith fragments. We refer readers to Figures 11C, 11D and 12B-D to view examples of organic matter 'lakes'.

Chalky Marl

The chalky marl lithology is the transitional lithology between pure chalk and dirty chalk or marl (Figure 18). They are brownish- to olive-grey and wispy-laminated to slightly bioturbated to massive. Chalky marls usually contain an abundance of flattened chalk pellets

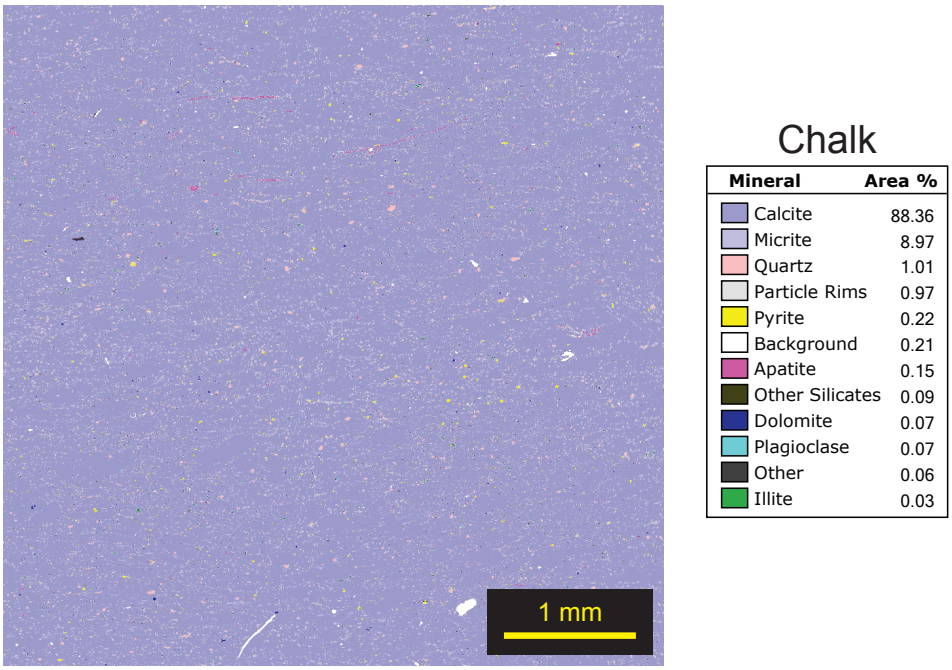

Figure 17. Representative mineralogy map of a 'B' chalk core sample (Well: Burbach 20-3H; Depth: 7193.5 ft. (2192.6 m)) acquired at 10 µm analysis resolution on the QEMSCAN®. Sample consists of almost entirely of calcite (calcite and micrite > 95%) Flattened chalk pellets exist but are difficult to distinguish from the micrite matrix.

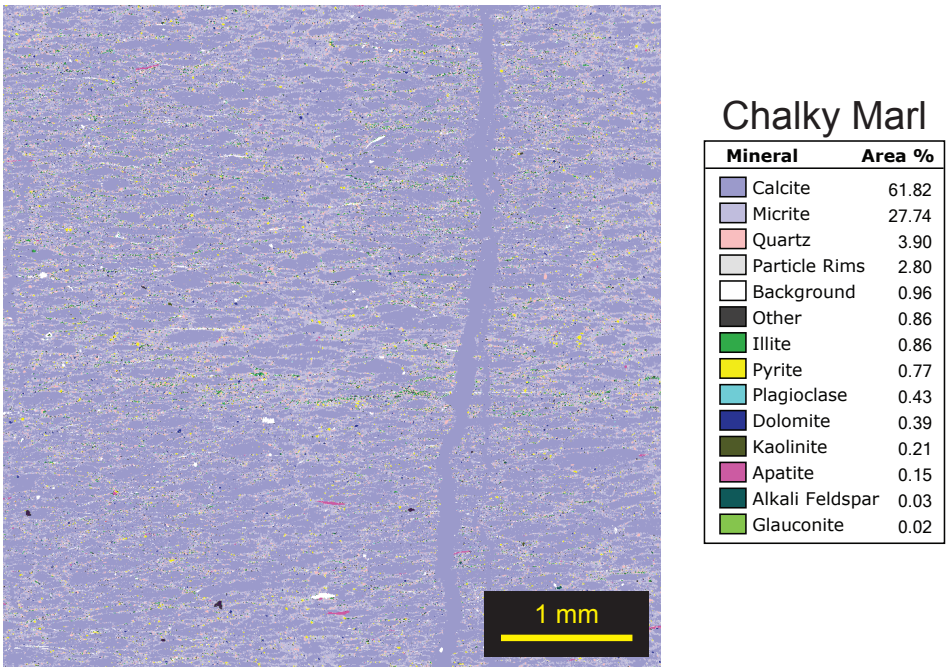

Figure 18. Representative mineralogy map of a 'B' chalky marl core sample (Well: T84X-31G Horse Creek Unit; Depth: 4202.5 ft. (1280.9 m)) acquired at 10 µm analysis resolution on the QEMSCAN®. Flattened chalk pellets are more easily distinguishable because the stark contrast between calcite (pellets) and micrite (matrix). The vertical calcite colored feature right of center is a calcite cemented microfracture which extended through the core several centimeters.

(65 to 85%) which float in a mixed micrite-grade skeletal particle and slightly silty, clay matrix (Longman et al., 1998). They also contain varying amounts of carbonate cement-filled planktonic foram tests, pyrite framboids, microstylolites and organic matter.

Marl

Marl deposition was strongly influenced by input of siliciclastic material from the west and cooler Arctic currents from the north (Sonnenberg, 2011b). These factors inhibited carbonate production and diluted carbonate sediment deposition across the basin. Niobrara marls in the DJ basin are generally dark brownish- or olive-grey and wispy to parallel laminated, but can be massive. Beds are composed of alternating laminae of clay and flattened chalk pellets in a slightly silty, clay-rich matrix (Figure 19). Chalk pellets are moderate to abundant and make up 35 to 65% of the rock (Longman et al., 1998). Foram tests can also be moderate to abundant and are filled with calcite cement, kaolinite clays, and pyrite. Oyster and inoceramid shell fragments

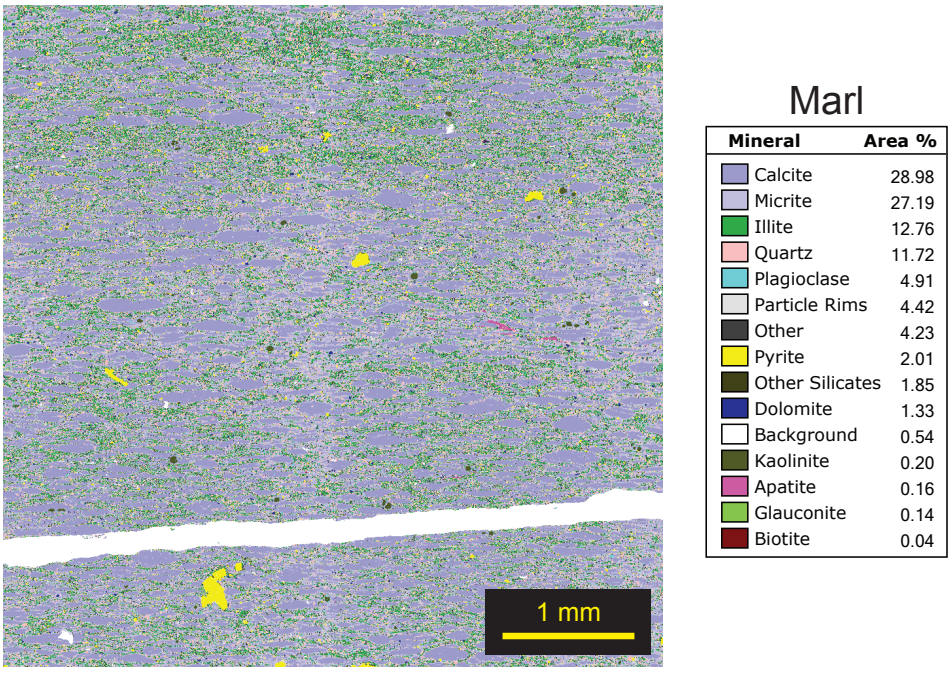

Figure 19. Representative mineralogy map of a 'B' marl core sample (Well: Lee 41-5; Depth: 7986.5 ft. (2434.3 m)) acquired at 10 µm analysis resolution on the QEMSCAN®. Flattened chalk pellets are very easily distinguishable because of the abundance of matrix micrite and clays. This sample also contains framboidal pyrite and clay-filled foram tests (kaolinite). The white horizontal feature is a mechanically induced fracture related to sample preparation.

are present locally. Pyrite framboids are common to abundant and regularly make up a few percent of a rock. The framboids are typically associated with matrix silts and clays. Microstylolites can be moderate to abundant and are thicker than in chalks and chalky marls, where more organic matter and undissolved solids are concentrated. Dissolution features are present. Organic matter is abundant in marl lithologies. It occurs commonly as large visible organic matter 'lakes', concentrated within microstylolites and in interparticle pores within chalk pellets.

Porosity Abundance

It is important to identify and understand the abundance and distribution of pore types within the Niobrara Formation since each contributes differently to permeability and thus, reservoir producibility. Because of similar constituents, each of the above lithologies contain similar pore types. However, each lithology differs in the way these pores connect and interact. Though good for hydraulic fracking because of its brittleness, a lithology that is excessively calcareous (pure chalk) may be overly cemented, effectually locking up most hydrocarbons and causing low flow rates to the induced fractures. Conversely, a lithology that is excessively argillaceous (pure marl) may contain an overabundance of clay minerals and organic matter that can clog pores and increase ductility, which in turn reduces the healing time of the induced fracture. It is also difficult to establish good hydraulic fractures in a lithology that is overly argillaceous. It would seem that chalky marl is the 'just right' lithology in terms of a balance between porosity, permeability, frackability and producibility.

CHALK DIAGENESIS

The principal components of chalk (i.e., coccoliths and foram tests) are composed of low-magnesium calcite, a chemically stable form of calcium carbonate under most near-sea-surface conditions (Lockridge and Scholle, 1978). However, during sediment settling and burial, chalk components and depositional textures undergo significant diagenetic transformation as a

consequence of physical and chemical changes (Pollastro and Scholle, 1986b). Hence, of the three main environments of diagenesis – marine, meteoric, and burial – the majority of chalk diagenesis and porosity modification takes place in the burial environment. Original chalk porosities of 60 to 80% are reduced to about 10% in the western DJ Basin where the Niobrara is most deeply buried and is most thermally mature (Pollastro and Scholle, 1986b). Examples of porosity loss and alteration in the Niobrara are illustrated in scanning electron micrographs (SEM) from samples representing shallow and deep burial depths in the DJ Basin (Figure 20).

Correct terminology for the significant phases of porosity evolution is an important part of a genetically oriented classification system. Here we recognize 11 porosity modifying terms of four types representing 1) the processes involved in porosity modification, 2) the direction and extent of modification, 3) the timing of modification, and 4) resulting porosity distribution. These four types and corresponding terms are listed in the summary diagram in Figure 21. These modifying terms relate specifically to the evolution of porosity in chalks and differ slightly from those proposed by Choquette and Pray (1970) though many of their terms are repeated here.

Modification Process

Mechanical Compaction. – Early porosity loss in chalks results from mechanical compaction associated with initial burial. This process includes compactional dewatering (reducing porosities by up to 50%), grain reorientation and grain breakage (Pollastro and Scholle, 1986b; Figures 20A and 20C). The process of chalk diagenesis in the Niobrara Formation has been extensively described by Scholle (1977), Lockridge and Scholle (1978), Precht and Pollastro (1985), Pollastro and Scholle (1986a), and Pollastro and Scholle (1986b). Dewatering, grain reorientation and breakage, and pressure solution of calcium carbonate at grain contacts and along pressure solution seams reduce chalk porosity sequentially with increasing burial depth. Thus, maximum burial is the main controlling factor in porosity and permeability loss in the Niobrara (Lockridge and Scholle, 1978).

Chemical Compaction and Dissolution. – Pressure solution features described as wispy

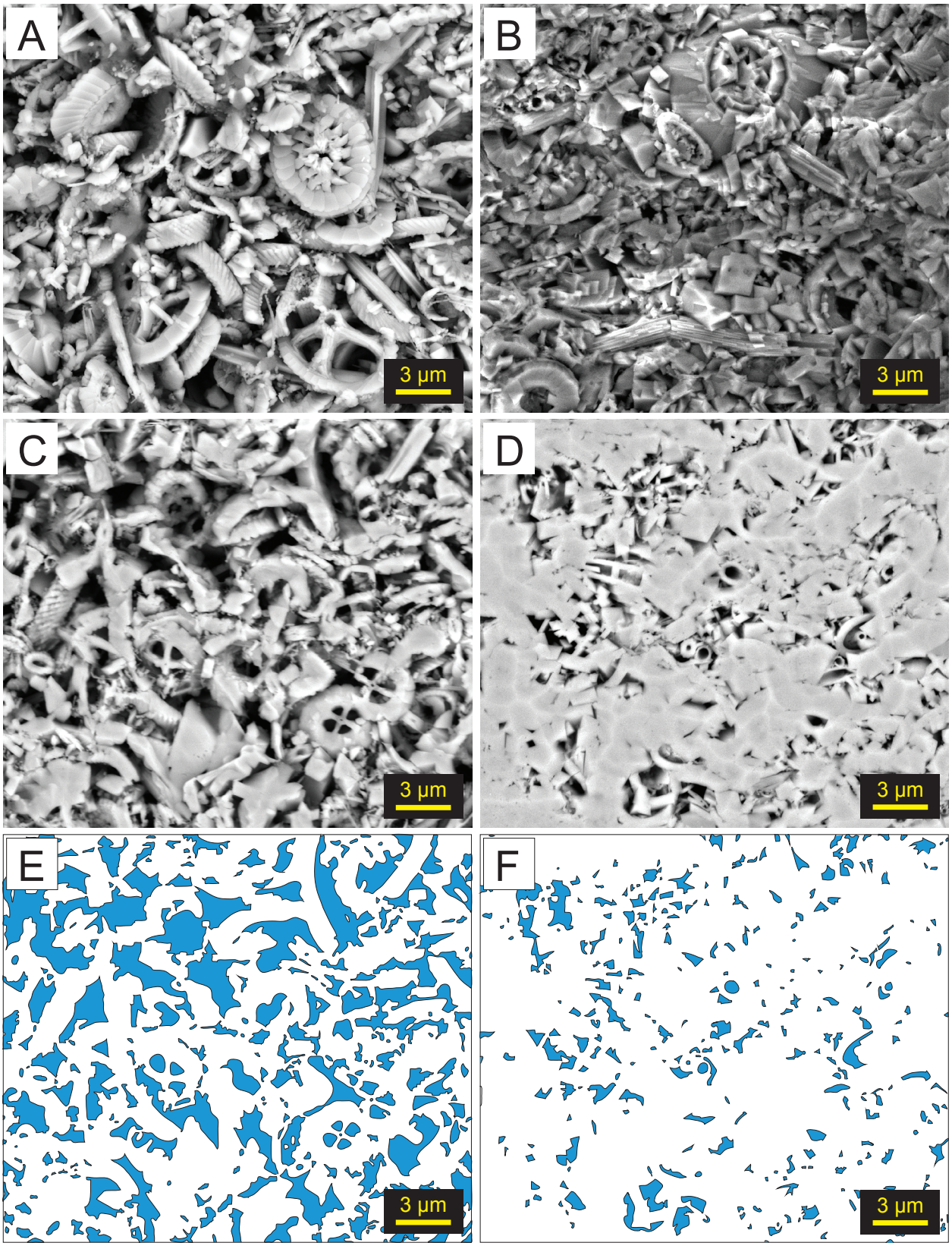

Figure 20. SEM photomicrograph comparison of Niobrara Formation chalks from core at different burial depths within the DJ Basin. Images A and C are the same sample from Sherman County, Kansas (Well: Schook-Errington 1; Depth: 1773.7 ft. (540.5 m)). Images B and D are the same sample from Weld County, Colorado (Well: Burbach 20-3H; Depth: 7193.5 ft. (2192.6 m)). Images A and B are unpolished while images C and D have been Ar-ion milled for better viewing of porosity. E and F are porosity illustrations correspond to the images above (E to C and F to D).

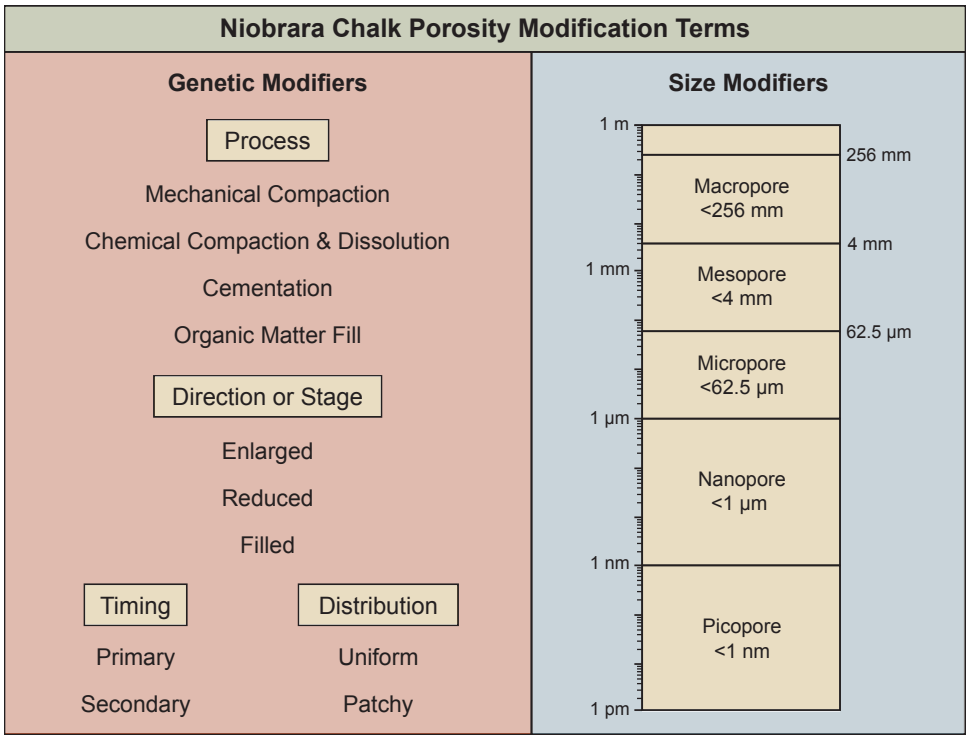

Figure 21. Chalk porosity modification term summary diagram. Genetic modifiers pertain to the timing of porosity formation, the processes involved in porosity modification, the direction and extent of porosity modification and the resulting porosity distribution. Pore-size modifiers include Macropores (< 256 mm), Mesopores (< 4 mm), Micropores (< 62.5 µm), Nanopores (< 1 µm), and Picopores (< 1nm). Figure is after Choquette and Pray (1970). The size modifiers diagram is modified from Loucks et al. (2012).

dissolution seams or microstylolites (Precht and Pollastro, 1985; Longman et al., 1998; Sonnenberg, 2011b) have been observed in thin section petrography, and SEM-based imaging (Figure 14). The origins of microstylolites in the Niobrara are well documented and are understood to form by chemical compaction and dissolution. (Precht and Pollastro, 1985; Pollastro and Scholle, 1986a; Longman et al., 1998). Most abundant in chalky marl and marl lithologies, they occur commonly throughout the Smoky Hill Member. They are best described

as sinuous and discontinuous, varying greatly in size, and commonly not extending entirely across a core, thin section or SEM sample width. Niobrara microstylolites lie subparallel to bedding planes and consist of insoluble residue concentrations of organic matter, partially dissolved foram tests and flattened chalk pellets, quartz silt, clays, pyrite, and other heavy minerals. The presence of these constituents suggests microstylolites are not artifacts created during core retrieval and decompression but represent original features preserved within the rock matrix.

Increasing compaction caused by further burial and increasing temperatures causes chemical compaction and dissolution of calcium carbonate at grain contacts and/or along pressure solution seams (Precht and Pollastro, 1985).

Cementation. – Cements precipitated in the burial environment are typically comprised of clear, low-magnesium sparry calcite enriched in Fe2+ and Mn2+. In typical (non-chalk) grain-rich limestone, these cements occur as 1) bladed, prismatic overgrowths of early, pore-lining cement crusts, 2) equicrystalline calcite mosaics filling interparticle pores, 3) drusy calcite mosaics with increasing crystal size toward pore centers, 4) coarse poikilotopic crystals that embay two or more grains, and/or 5) syntaxial overgrowths. In the Niobrara 'B' chalk, clear sparry cements are limited to drusy infilling of intraparticle pores within forams, coccospheres, and calcispheres. The vast majority of calcium carbonate liberated by pressure dissolution is reprecipitated locally as cement overgrowths (in crystallographic continuity) on coccolith plates and crystallites (Precht and Pollastro, 1985; Figures 20B and 20D). Syntaxial cements increase the size of particles while retaining or enhancing the rhombic shape. Cementation also results in welding of grains and solidification of the chalk. Pores are reduced in size, but retain angular morphologies (Figures 20D and 20F).

Organic Matter Fill. – Organic matter fill is included as a process because of the extensive amount of organic matter-filled pores observed in coccolith-rich fecal pellets. It is unclear if the organic matter is primary or if it was moved into the pellets during burial and compaction.

Modification Direction

Porosity modification or extent is represented by three modifying terms, enlarged, reduced and filled. Enlarged and reduced are the main direction terms, and filled is the frequently encountered end stage of porosity reduction. Enlarged is normally used to represent enlargement by solution. It is applied only to modifications that do not obliterate the identity of the original pore. Reduced is used for stages of porosity reduction between the initial state and the end stage of filled. Filled is commonly very useful in description and interpretation of the porosity evolution of nonporous carbonate rocks, which are much more common than porous carbonates. These terms are best used with the notation of process, but can also be used independently.

Pore Distribution

Pore distribution is a relatively new element in porosity classification and has been shown by Lønøy (2006) to have a significant influence on porosity/permeability relationships. The distribution of the various pore types found in a sample can be classified as either uniform or patchy (Figure 22). In the Niobrara, pore distribution is greatly affected by the abundance of chalk pellets relative to the matrix (micrite-grade chalk-rich vs. clay-rich). In chalk and chalky marl lithologies where chalk pellets are plentiful in a micrite-rich matrix, corresponding porosity distributions are more uniform (Figures 22A and 22B). Chalky marl and marl lithologies that contain fewer chalk pellets in a quartz silt and clay-rich matrix have a more patchy distribution (Figures 22C and 22D). Individual chalk pellets are also greatly affected by the surrounding matrix. More porosity within chalk pellets appears to be preserved in a micrite-rich chalk matrix where mechanical and chemical compaction occur differently than in a quartz silt and clay-rich matrix (Figures 22A and 22C).

Pore-Size Modifiers

The pore size modifiers presented in Choquette and Pray's 1970 porosity classification provided a useful pore size classification for carbonate rocks. Their classification included

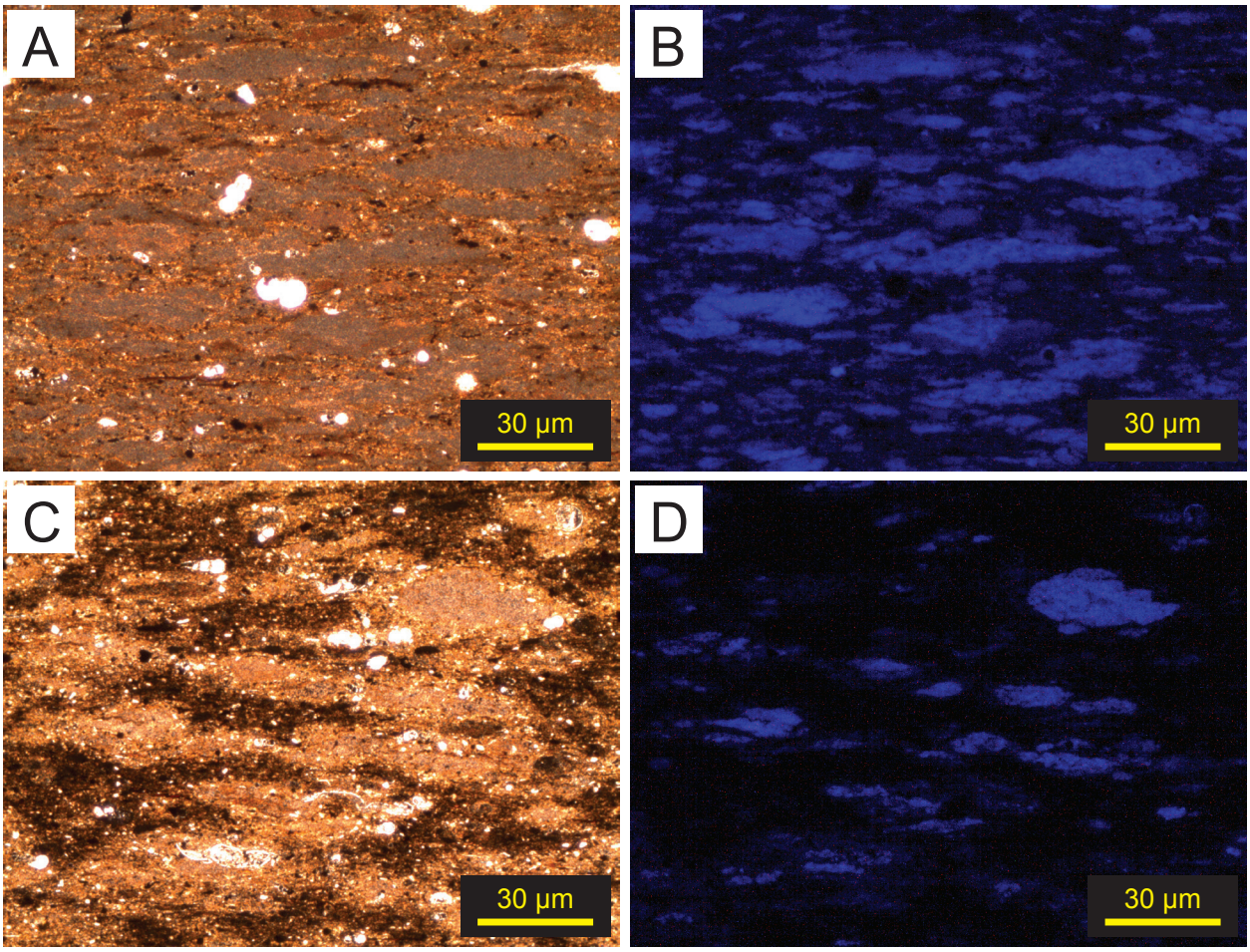

Figure 22. Thin section photomicrographs viewed under plain transmitted light (A and C) and ultra violet (UV) light (B and D) comparing uniform and patchy porosity distributions in the Niobrara. (A and B) Chalk lithology consisting of flattened chalk pellets and foram tests in a micrite-dominated matrix. (C and D) Marl lithology consisting of flattened chalk pellets, foram tests, pyrite and organic matter in a clay-dominated matrix.

megapores (4 to 256 mm), mesopores (62.5 µm to 4 mm) and micropores (anything less than 62.5 µm). No further subdivisions of pores smaller than 62.5 microns was made. In their work classifying pores in mudstones, Loucks et al. (2012) recognized the upper pore size is generally much less than 62.5 microns. Because pores in mudstone commonly range from a few nanometers to several micrometers in diameter, they believed it would be useful to have well-defined size classes for pores of that size range. Thus, they further subdivided Choquette and Pray's (1970) micropore size class into micropores (62.5 to 1 µm), nanopores (less than 1 µm to 1 nm) and picopores (less than 1 nm). These subdivisions are included in the size modifiers

portion of the porosity modification terms diagram in Figure 21.

CONCLUSIONS

Current emphasis on unconventional reservoirs has created a need for a more complete understanding of microporosity and effective permeability pathways within Cretaceous chalk reservoirs. Still in early stages of study and development, the Niobrara Formation in the Denver-Julesburg (DJ) Basin is an emergent oil and natural gas producing play in low permeability chalk and marl sequences.

Integration of depositional fabric with pore-type distribution highlights the unique textural and depositional nature of chalk and provides a starting point for the evaluation of diagenetic porosity modification. New terms relating chalk depositional textures include two main divisions: Rainstone comprises chalk that result from settling of planktonic skeletal remains and fecal pellets via marine snow in the water column. Terms related to rainstone textures are pelagic mudstone, pelagic wackestone, and pelagic packstone. Allochthonous chalks consist of rocks formed by gravity-induced, redeposition of pelagic carbonate sediments. Terms related to allochthonous chalk textures are allomudstone, allofloatstone, and allorudstone. Niobrara chalks, the Austin Chalk, and many of the North Sea Chalks are predominantly rainstone. Chalks in the North Sea Central Graben are predominantly allochthonous chalks.

Niobrara chalk micropores are different than conventional carbonate reservoir pores. The chalk porosity classification using scanning electron micrograph (SEM) images is based on pore types observed in the Niobrara. Consisting of four major pore types, and ten subtypes, this system can be used to quantify pores and relate them to depositional texture, pore networks, diagenetic history, and porosity distribution. The four pore-type classes are 1) interparticle pores occurring between mineral particles, 2) intraparticle pores within mineral particles, 3) intraparticle organic matter pores, and 4) channel pores. Within the main Niobrara reservoir lithologies, pore type is strongly influenced by the relative abundance of chalk pellets. In lithologies where chalk pellets are common, a strong intraparticle pore network is observed.

Where chalk pellets are rare, the pore network becomes strongly interparticle.

Niobrara reservoir lithologies vary greatly across the DJ Basin between chalk, chalky marl, and marl. This variation is a function of the abundance of chalk pellets relative to the matrix (micrite-rich vs. quartz silt- and clay-rich). Pure chalk may be overly cemented while clay and organic matter in pure marl may clog pores and increase formation ductility. Chalky marl is thought to be the best reservoir lithology in terms of balance between porosity, permeability, frackability and producibility.

During sediment settling and burial, chalk components and depositional textures undergo significant diagenetic transformation. We recognize 11 modifying terms of four types representing process, direction, timing, and distribution of porosity alteration. The majority of change and porosity modification takes place in the burial environment where pore shape and abundance are modified by mechanical compaction, chemical compaction and dissolution, syntaxial cement overgrowths, and organic matter fill. Maximum burial depth is the main controlling factor in Niobrara porosity and permeability loss in the DJ Basin. Porosity distribution is controlled by the presence of chalk pellets and the mineralogy of the matrix. Similarly, permeability is a function of matrix lithology.

The modified Dunham (1962) classification of chalk depositional textures is not intended to be Niobrara specific. It was created after extensive research related to the Niobrara, as well as the Austin and North Sea chalks and great effort has been made to incorporate depositional and textural information gleaned from a wide range of sources. We believe this classification is applicable to the formations mentioned previously, together with all other chalk formations. We do not advocate disuse of the term chalk. Instead, we encourage those who study chalk deposits to use this scheme as a tool of clarification when conditions require distinction between the texture and origin of specific rock types.

REFERENCES CITED

Alam, M. M., M. K. Borre, I. L. Fabricius, K. Hedegaard, B. Rogen, Z. Hossain, and A. S. Krogsboll, 2010, Biot's coefficient as an indicator of strength and porosity reduction: Calcareous sediments from Kerguelen Plateau: Journal of Petroleum Science and Engineering, v. 70, p. 282-297.

Alldredge, A. L., and M. W. Silver, 1988, Characteristics, dynamics, and significance of marine snow: Progress in Oceanography, v. 20, p. 41-82.

Anderskouv, K. and F. Surlyk, 2011, Upper Cretaceous chalk facies and depositional history recorded in the Mona-1 core, Mona Ridge, Danish North Sea: Geological Survey of Denmark and Greenland Bulletin, v. 25, 63 p.

Anderskouv, K., and F. Surlyk, 2012, The influence of depositional processes on the porosity of chalk: Journal of the Geological Society, London, v. 169, p. 311-325.

Ayling, B., P. Rose, S. Petty, E. Zemach, and P. Drakos, 2012, QEMSCAN® (Quantitative Evaluation of Minerals by Scanning Electron Microscopy): Capability and application to fracture characterization in Geothermal Systems: Proceedings of the 37th Workshop on Geothermal Reservoir Engineering, January 30-February 1, Stanford University, Stanford, California.

Barlow, L. K., and E. G. Kaufman, 1985, Depositional cycles in the Niobrara Formation, Colorado Front Range, in L. M. Pratt, E. G. Kauffman and F. B. Zelt, (eds.), Fine-grained deposits and biofaces of the Cretaceous Western Interior Seaway – Evidence of Cyclic Sedimentary Processes: SPEM Field Trip Guidebook, v. 4, p. 199-208.

Borre, M. K., and I. L. Fabricius, 1998, Chemical and mechanical processes during burial diagenesis of chalk: an interpretation based on specific surface data of deep-sea sediments: Sedimentology, v. 45, no. 4, p. 755-769.

Brace, W. F., E. Silver, K. Hadley, and C. Goetze, 1972, Cracks and pores: A closer look: Science, v. 178, p. 162-163.

Choquette, P. W., and L. C. Pray, 1970, Geologic nomenclature and classification of porosity in

sedimentary carbonates: AAPG Bulletin, v. 54, no. 2, p. 207-250.

Cobbold, P. R., A. Zanella, N. Rodrigues, and H. Løseth, 2013, Bedding-parallel fibrous veins (beef and cone-in-cone): Worldwide occurance and possible significance in terms of fluid overpressure, hydrocarbon generation and mineralization: Marine and Petroleum Geology, v. 43, p. 1-20.

Driskill, B., J. Walls, S. W. Sinclair, and J. DeVito, 2013, Applications of SEM imaging to reservoir characterization in the Eagle Ford Shale, south Texas, U.S.A., in W. Camp, E. Diaz, and B. Warak, (eds.), Electron microscopy of shale hydrocarbon reservoirs: AAPG Memoir 102, p. 115-136.

Dunham, R. J., 1962, Classification of carbonate rocks according to depositional texture, in W. E. Ham, (ed.), Classifiaction of cabonate rocks–a symposium: AAPG Memoir 1, p. 108-121.

Embry, A. F., and J. E. Klovan, 1971, A Late Devonian reef tract on northeastern Banks island, N.W.T.: Bulletin of Canadian Petroleum Geology, v. 19, no. 4, p. 730-781.

Fabricius, I. L., 2007, Chalk: composition, diagenesis and physical properties: Bulletin of the Geological Society of Denmark, v. 55, p. 97-128.

Flügel, E., 2004, Microfacies analysis of limestones, Berlin, Springer-Verlag, 633 p.

Gustason, G., and M. Deacon, 2010, Niobrara stratigraphy & shale resource, DJ Basin: PTTC Field Trip Guidebook, p. 104.

Hardman, R. F. P., 1982, Chalk reservoirs of the North Sea: Geological Society of Denmark Bulletin, v. 30, p. 119-137.

Hassenkam, T., A. Johnson, K. Bechgaard, and S. L. S. Stipp, 2011, Tracking single coccolith dissolution with picogram resolution and implications for CO_2 sequestration and ocean acidification: Proceedings of the National Academy of Sciences of the United States of America, v. 108, no. 21, p. 8571-8576.

Hattin, D. E., 1975, Petrology and origin of fecal pellets in Upper Cretaceous strata of Kansas and Saskatchewan: Journal of Sedimentary Petrology, v. 45, no. 3, p. 686-696.

Hatton, L. R., 1986, Geometry of allochthonous Chalk Group members, Central Trough, North

Sea: Marine Petroleum Geology, v. 3, no. 2, p. 79-98.

Herrington, P. M., K. Pederstad, and J. A. D., Dickson, 1991, Sedimentology and diagenesis of resedimented and rhythmically bedded chalks from the Eldfisk Field, North Sea Central Graben: AAPG Bulletin, v. 75, no. 11, p. 1661-1674.

Ineson, J. R., B. Buchardt, S. Lassen, J. A., Rasmussen, P. Schioler, N. H., Schovsbo, E. Sheldon, and F. Surlyk, 2006, Stratigraphy and palaeoceanography of upper Maastrichtian chalk, southern Danish Central Graben: Geological Survey of Denmark and Greenland Bulletin, v. 10, p. 9-12.

Ings, S. J., R. A. MacRae, J. W. Shimeld, and G. Pe-Piper, 2005, Diagenesis and porosity reduction in the Late Cretaceous Wysndot Formation, offshore Nova Scotia: a comparison with Norwegian North Sea chalks: Bulletin of Canadian Petroleum Geology, v. 53, no. 3, p. 237-249.

Jarvie, D. M., R. J. Hill, T. E. Ruble, and E. M. Pollastro, 2007, Unconventional shale-gas systems: The Mississippian Barnett Shale of north-central Texas as one model for thermogenic shale-gas assessment: AAPG Bulletin, v. 91, no. 4, p. 475-499.

Kauffman, E. G., and W. G. E. Caldwell, 1993, The Western Interior Basin in space and time, in W. G. E. Caldwell and E. G. Kauffman, (eds.), Evolution of the Western Interior Basin: Geological Association of Canada Special Paper 39, p. 1-30.

Kennedy, W. J., 1987, Sedimentology of Late Cretaceous-Paleocene chalk reservoirs, North Sea Central Graben, in, Brooks, J. and K. Glennie, (eds.), Petroleum Geology of North West Europe. Graham and Trotman, London, p. 469-481.

Landon, S. M., M. W. Longman, and B. A. Luneau, 2001, Hydrocarbon source rock potential of the Upper Cretaceous Niobrara Formation, Western Interior Seaway of the Rocky Mountain region: The Mountain Geologist, v. 38, p. 1-18.

Lockridge, J. P., and P. A. Scholle, 1978, Niobrara gas in eastern Colorado and northwestern Kansas, in J. D. Pruit ad P. E. Coffin, (eds.), Energy resources of the Denver basin: Rocky Mountain Association of Geologists, Symposium Guidebook, p. 35-49.

Longman, M. W., B. A. Luneau, and S. M. Landon, 1998, Nature and distribution of Niobrara lithologies in the Cretaceous Western Interior Seaway of the Rocky Mountain Region: The Mountain Geologist, v. 35, no. 4, p. 137-170.

Lønøy, A., 2006, Making sense of carbonate pore systems: AAPG Bulletin, v. 90, no. 9, p. 1381-1405.

Loucks, R. G., R. M. Reed, S. C. Ruppel, and U. Hammes, 2012, Spectrum of pore types and networks and a descriptive classification for matrix-related mudrock pores: AAPG Bulletin, v. 96, no. 6, p. 1071-1098.

Loucks, R. G., R. M. Reed, S. C. Ruppel, and D. M. Jarvie, 2009, Morphology, genesis, and distribution of nanometer-scale pores in siliceous mudstones of the Mississippian Barnett Shale: Journal of Sedimentary Research, v. 79, p. 848-861.

Lowe, D. R., 1982, Sediment gravity flows: II. Depositional medels with special reference to the deposits of high-density turbidity currents: Journal of Sedimentary Petrology, v. 52, no. 1, p. 279-297.

Lucia, F. J., 1983, Petrophysical parameters estimated from visual descriptions of carbonate rocks: A field classification of carbonate pore space: Journal of Petroleum Technology, v. 216, p. 221-224.

Lucia, F. J., 1995, Rock-fabric/petrophysical classification of carbonate pore space for reservoir characterization: AAPG Bulletin, v. 79, no. 9, p. 1275-1300.

Lucia, F. J., 1999, Carbonate reservoir characterization: Berlin, Springer-Verlag, 226 p.

Mei, M. X., 2007, Revised classification of microbial carbonates: complementing the classification of limestones: Earth Science Frontiers, v.14, no. 5, p. 222-232.

Milliken, K. L., M. Rudnicki, D. N. Awwiller, and T. Zhang, 2013, Organic matter-hosted pore system, Marcelleus Formation (Devonian), Pennsylvanian: AAPG Bulletin, v. 97, no. 2, p. 177-200.

Pollastro, R. M., and P. A. Scholle, 1986a, Diagenetic relationships in a hydrocarbon-productive chalk – the Cretaceous Niobrara Formation, in F. A. Mumpton, (ed.), Studies in

diagenesis, USGS Bulletin 1578, p. 219-236.

Pollastro, R. M., and P. A. Scholle, 1986b, Exploration and development of hydrocarbons from low-permeability chalks – an example from the Upper Cretaceous Niobrara Formation, Rocky Mountain Region, in C. W. Spencer, and R. F. Mast, (eds.), Geology of tight gas reservoirs, AAPG Studies in Geology 24, p. 129-141.

Precht, W. F., and R. M. Pollastro, 1985, Organic and inorganic constituents of the Niobrara Formation in Weld County, Colorado, in L. M. Pratt, E. G. Kauffmann, and F. B. Zelt, (eds.), Fine-grained deposits and biofacies of the Cretaceous Western Interior Seaway, Evidence of cyclic sedimentary processes: SEPM Second Annual Midyear Meeting, Golden, Colorado, Field Trip Guidebook no. 9, p. 223-249.

Schlager, W., 2000, Sedimentation rates and growth potential of tropical, cool-water and mud-mound carbonate systems: Geological Society of London, Special Publications, v. 178, no. 1, p. 217-227.

Schlager, W., 2003, Benthic carbonate factories of the Phanerozoic: International Journal of Earth Sciences, v. 92, no. 4, p. 445-464.

Schlager, W., 2005, Carbonate sedimentology and sequence stratigraphy: SEPM Concepts in Sedimentology and Paleontology Series, v. 8, 208 p.

Scholle, P. A., 1977, Chalk diagenesis and its relation to petroleum exploration: Oil from chalks, a modern miracle?: AAPG Bulletin, v. 61, no. 7, p. 982-1009.

Simmons, G., and D. Richter, 1976, Microcracks in Rocks, in R. J. G. Strens, (ed.), The physics and chemistry of minerals and rocks, Wiley-Interscience, New York, p. 105-137.

Slatt, R. M., and N. R. O'Brien, 2011, Pore types in the Barnett and Woodford gas shales: Contribution to understanding gas storage and migration pathways in fine-grained rocks: AAPG Bulletin, v. 95, no. 12, p. 2017-2030.

Sonnenberg, S. A., 2011a, Petroleum geology of Silo Field, Wyoming: AAPG Rocky Mountain Section Meeting, Cheyenne, Wyoming, June 25-29: Search and Discovery Article #20115.

Sonnenberg, S. A., 2011b, The Niobrara Petroleum System: A new resource play in the Rocky Mountain Region, in J. E. Estes-Jackson, and D. S. Anderson, (eds.), Revisiting and Revitalizing the Niobrara in the Central Rockies, Rocky Mountain Association of Geologists, Denver, CO, p. 13-32.

Sprunt, E. S., and W. F. Brace, 1974, Direct observation of microcavities in crystalline rocks: International Journal of Rock Mechanics and Mining Sciences & Geomechanics Abstracts, v. 11, no. 4, p. 139-150.

Thierstein, H. R., 1980, Selective dissolution of Late Cretaceous and Earliest Tertiary calcareous nannofossils: experimental evidence: Cretaceous Research, v. 1, no. 2, p. 165-176.

Van der Molen, A. S., H. W. Dudok van Heel, and T. E. Wong, 2005, The influence of tectonic regime on chalk deposition: examples of the sedimentary development and 3D-seismic stratigraphy of the Chalk Group in the Neatherlands offshore area: Basin Research, v. 17, p. 63-81.

Watts, N. L., J. F., Lapre, F. S., Van Schijndel-Goester, and A. Ford, 1980, Upper Cretaceous and Lower Tertiary chalks of the Albuskjell area, North Sea: deposition in a base-of-slope environment: Geology, 8, p. 217-221.

Williams, P., and D. Lyle, 2011, Bring in the rigs, in J. E. Estes-Jackson, and D. S. Anderson, (eds.), Revisiting and Revitalizing the Niobrara in the Central Rockies, Rocky Mountain Association of Geologists, Denver, CO, p. 33-46.